A versatile *in vivo* system for directed dissection of gene expression patterns

Daryl M Gohl[1], Marion A Silies[1], Xiaojing J Gao[2], Sheetal Bhalerao[1], Francisco J Luongo[1], Chun-Chieh Lin[3], Christopher J Potter[3] & Thomas R Clandinin[1]

Tissue-specific gene expression using the upstream activating sequence (UAS)–*GAL4* binary system has facilitated genetic dissection of many biological processes in *Drosophila melanogaster*. Refining *GAL4* expression patterns or independently manipulating multiple cell populations using additional binary systems are common experimental goals. To simplify these processes, we developed a convertible genetic platform, the integrase swappable *in vivo* targeting element (InSITE) system. This approach allows *GAL4* to be replaced with any other sequence, placing different genetic effectors under the control of the same regulatory elements. Using InSITE, *GAL4* can be replaced with *LexA* or *QF*, allowing an expression pattern to be repurposed. *GAL4* can also be replaced with *GAL80* or split-*GAL4* hemi-drivers, allowing intersectional approaches to refine expression patterns. The exchanges occur through efficient *in vivo* manipulations, making it possible to generate many swaps in parallel. This system is modular, allowing future genetic tools to be easily incorporated into the existing framework.

Many *in vivo* manipulations rely on directing gene expression to a specific tissue or to a particular developmental time. There are two basic methods to do this. In one approach, transposable elements carrying genetic effectors with minimal promoters are inserted into the genome, and expression is driven by local gene regulatory elements[1,2]. Alternatively, regulatory elements can be fused to genetic effectors *in vitro* and reinserted in the genome[3–5]. Such enhancer traps and enhancer fusions have been powerful tools in cell biology, development, physiology and neuroscience[6–9].

In *Drosophila melanogaster,* the upstream activating sequence (UAS)-*GAL4* system allows for expression of UAS-linked genes in cells expressing the transcription factor *GAL4* (ref. 1). Two additional binary systems, using the *LexA* and *QF* transcriptional activators, allow independent manipulation of multiple populations of cells[10,11]. However, although many enhancer trap and enhancer fusion lines exist, particularly for the UAS-*GAL4* system, the expression of such lines is seldom confined to a single tissue or cell type, limiting the resolution of these approaches[4,12,13].

Several strategies exist for using the intersections of partially overlapping expression patterns to generate increased specificity. For example, *FLP*, *GAL4* and *QF* have been used with *FRT*-flanked interruption or flip-out cassettes to target subsets of expression patterns[11,13–15]. The split-*GAL4* system allows *GAL4* activity to be reconstituted in cells that express both halves of the hemi-driver[16]. Finally, the *GAL80* repressor can be used to subtract the overlap between two expression patterns[12,17]. Though these intersectional methods are useful for generating lines with more specific gene expression patterns, a drawback of these approaches is that with each elaboration or extension of the *GAL4* system, new combinations of these regulatory elements or their reporters frequently need to be designed and, in the worst case, whole libraries need to be regenerated.

Recombinase-mediated cassette exchange (RMCE) methods allow a sequence cassette to be replaced *in vivo*. Several strategies for RMCE, typically using a microinjected plasmid as the substrate for cassette exchange, have been developed[18–24]. Several of these approaches rely on Flp recombinase–mediated recombination using wild-type or mutant *FRT* sites to target an *FRT*-flanked cassette to a specific locus[20,21,23]. Another uses Cre recombinase and a pair of incompatible *loxP* sites[22]. The *Streptomyces* phage ΦC31 integrase, which catalyzes irreversible site-specific recombination between two sites (*attP* and *attB*)[25,26], has had a profound impact on animal transgenesis and has made possible several new RMCE strategies[18,19].

We combined these recombination systems into a versatile platform to facilitate the segmentation of complex expression patterns and to allow *GAL4* expression patterns to be repurposed. The integrase swappable *in vivo* targeting element (InSITE) system allows an enhancer trap or enhancer fusion to be rapidly converted from *GAL4* to any other sequence (**Fig. 1a**). The InSITE system uses an RMCE strategy in which the substrate for RMCE can be genetically derived, allowing replacement of *GAL4* simply by crossing flies. We demonstrate that such swaps can be done either entirely genetically, using genomic donor lines, or with a microinjected donor plasmid. As this strategy is highly efficient, it is possible to perform high-throughput swapping of many enhancer trap

[1]Department of Neurobiology, Stanford University, Stanford, California, USA. [2]Department of Biological Sciences, Stanford University, Stanford, California, USA. [3]Department of Neuroscience, The Johns Hopkins University School of Medicine, Baltimore, Maryland, USA. Correspondence should be addressed to T.R.C. (trc@stanford.edu).

RECEIVED 19 NOVEMBER 2010; ACCEPTED 17 DECEMBER 2010; PUBLISHED ONLINE 30 JANUARY 2011; DOI:10.1038/NMETH.1561

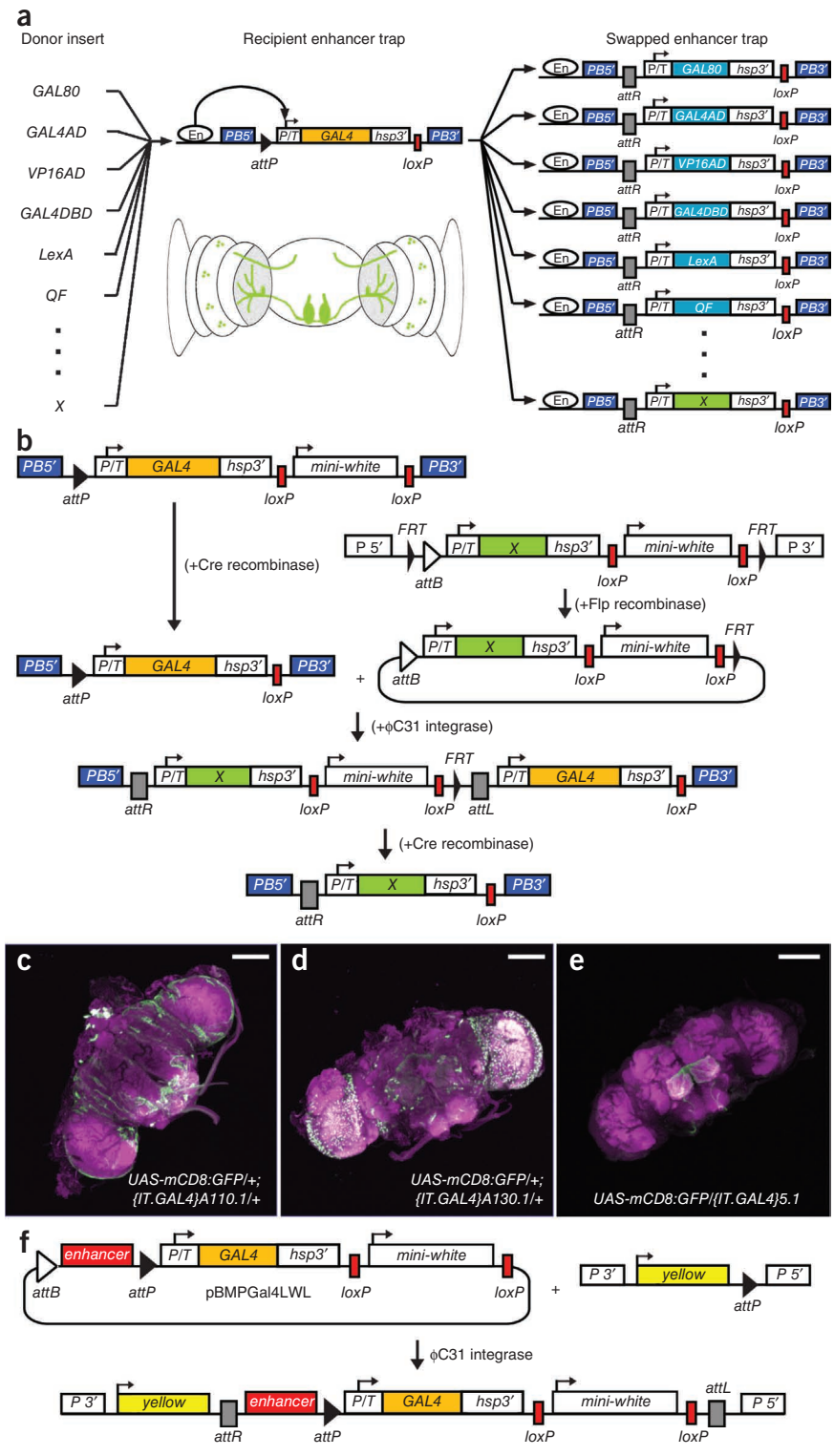

Figure 1 | The InSITE system. (**a**) Schematic illustration of the InSITE system, which can be used to convert a *GAL4* enhancer trap to another sequence, *X*, which will then be expressed under the control of local enhancers (En). P/T, P transposase promoter; PB, piggyBac transposon. (**b**) Schematic illustration of the procedure for genetically swapping *GAL4* with sequence *X*. (**c**–**e**) Fluorescence images showing the results of an immunohistochemical analysis of InSITE enhancer trap expression in the adult brain: *P* element line *P{IT.GAL4}A110.1* (**c**), *P* element line *P{IT.GAL4}A130.1* (**d**) and *PiggyBac* line *PBac{IT.GAL4}5.1* (**e**). Green, anti-mCD8; magenta, anti-Bruchpilot. Scale bars, 100 µm. (**f**) Schematic illustrating the insertion of the InSITE-compatible enhancer fusion vector, pBMPGal4LWL into a genomic *attP* site.

lines to multiple different effector molecules in parallel. In addition, we describe an enhancer fusion vector that is compatible with this replacement strategy, allowing a single transgene to be diversified *in vivo*. Finally, because the InSITE system allows *GAL4* to be converted into any other sequence, this platform is forward-compatible with currently unanticipated future technologies.

RESULTS

A convertible enhancer-trap platform

The InSITE enhancer trap contains a minimal (P transposase) promoter, the *GAL4* transcriptional activator and an *attP* recognition sequence for ΦC31 integrase[18,19,25,26] (**Fig. 1b**). We constructed swappable enhancer traps using two different transposons, the *Drosophila melanogaster*–specific *P* element and the *piggyBac* element, which has been used to transform a wide range of species, from insects to mammals[27–30] (**Supplementary Fig. 1**). *PiggyBac* elements also have a different insertion spectrum from *P* elements, facilitating the generation of lines with distinct expression patterns[31]. We established transformants and identified mobile, X chromosome–linked insertions, which allow the isolation of additional lines for enhancer-trap screens, for both transposons. Both the *P* element and *piggyBac* transposons (referred to as *P{IT.GAL4}* and *PBac{IT.GAL4}*, respectively, in which *IT* denotes InSITE target) functioned as enhancer traps and were expressed in diverse patterns in the adult brain (**Fig. 1c–e** and **Supplementary Fig. 2**).

The InSITE system uses three site-specific recombinases to exchange *GAL4* with any other sequence[19] (**Fig. 1b**). First, we treated the original enhancer trap with Cre recombinase, which removes the *loxP*-flanked *mini-white* marker[32]. Next, we introduced an *FRT*-flanked genomic donor line together with transgenes expressing Flp recombinase and ΦC31 integrase. In a strategy similar to that used to generate knockout alleles[33], upon treatment with Flp recombinase, a circular, *attB*-containing molecule is excised from the donor chromosome (**Fig. 1b**). Targeting of a genomic *FRT*-flanked cassette to a second *FRT*-containing locus using Flp recombinase has been previously described[20]. We reasoned that the irreversible nature of ΦC31 integrase–mediated insertion would allow for high-efficiency re-integration of the Flp

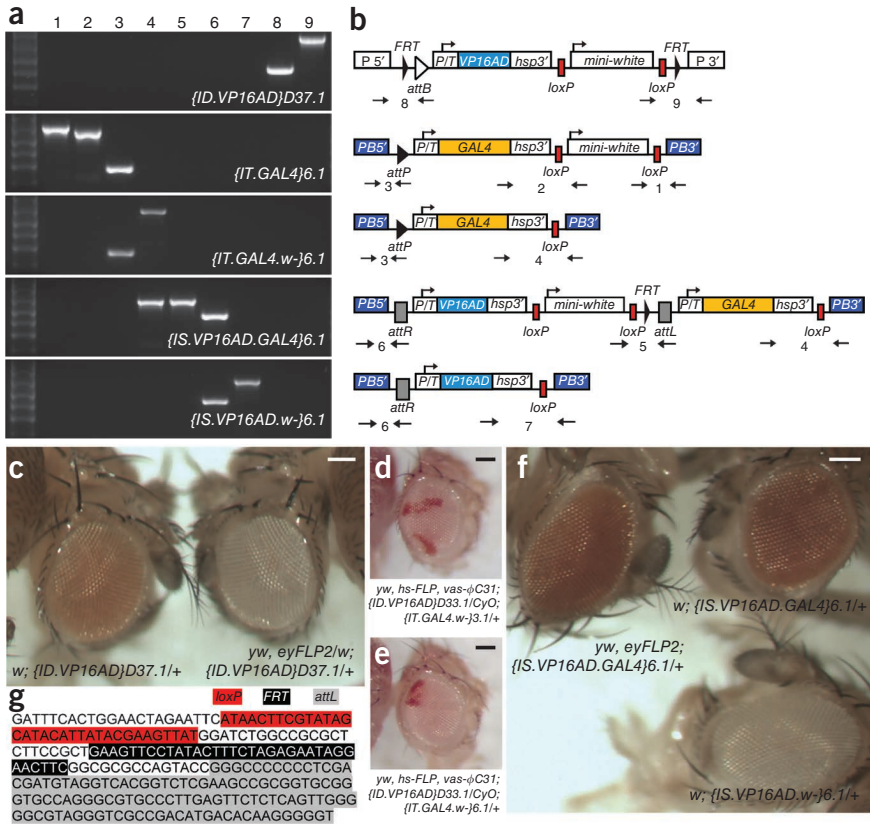

Figure 2 | Molecular and genetic validation of the enhancer-trap exchange. (**a**,**b**) Results of PCR analyses (**a**) to confirm each step of the genetic conversion of line *PBac{IT.GAL4}6.1* to the *VP16AD* hemi-driver, with amplicons numbered as in schematics in **b**. Locations of PCR primers are shown under each construct. (**c**) Images of flies with *P{ID.VP16AD}D37.1/+* (left) and *y, w, eyFLP2; P{ID.VP16AD}D37.1/+* (right), showing that genetic donor constructs lose *mini-white* expression when crossed to *eyFLP2*. (**d**–**e**) Images of heat-shocked adult flies carrying the InSITE donor and recipient transgenes, as well as *hs-FLP* and *vas-ΦC31 integrase* transgenes. (**d**) *y, w* (*yw*), *hs-FLP, vas-ΦC31; P{ID.VP16AD}D33.1/CyO; PBac{IT.GAL4.w-}3.1/+*. (**e**) *y, w, hs-FLP, vas-ΦC31; P{ID.VP16AD}D33.1/CyO; PBac{IT.GAL4.w–}6.1/+*. (**f**) *mini-white* expression in *w; PBac{IS.VP16AD.GAL4}6.1/+* (top right), *w; PBac{IS.VP16AD.w-}6.1/+*, (bottom) and *y, w, eyFLP2; PBac{IS.VP16AD.GAL4}6.1/+* (top left) flies. Scale bars, 100 μm. (**g**) Sequence of the PCR product of primer pair 5, including the *loxP*, *FRT* and *attL* sites.

recombinase–liberated donor molecule into the *attP* site of the InSITE enhancer trap (**Fig. 1b**). Integration events can be detected by the reappearance of the *mini-white* marker. Both constructs contain *loxP* sites oriented such that when treated with Cre recombinase, the original *GAL4* and *mini-white* marker in the integrated donor are deleted, leaving just the donor sequence. Thus, *GAL4* can be replaced with any other sequence, which should then be expressed under the control of the same regulatory elements.

In addition to the purely genetic swap, a microinjected plasmid analogous to the circular molecule that is liberated by Flp recombinase can also be integrated into the *attP* site of the enhancer trap (**Supplementary Fig. 3**). A similar strategy using a microinjected *LexA* donor plasmid has recently been described[24].

An InSITE-compatible enhancer fusion vector

Another approach to segmenting complex expression patterns is to use enhancer fusion constructs, in which a DNA fragment corresponding to an endogenous regulatory region is cloned upstream of *GAL4* or another effector. This approach has the advantage that lines containing enhancer subfragments are often expressed in fewer cells than enhancer traps, and enhancers can be further subdivided *in vitro* or the effector molecule can be switched by generating new constructs[4]. To take advantage of the enhancer fusion approach but bypass the need to clone and microinject each new construct, we made an InSITE-compatible enhancer fusion vector (**Fig. 1f**). We cloned an enhancer fragment with a known expression pattern, *ortc2* (ref. 34), into this vector and inserted this construct into the *attP2* landing site[25] and one of the Cre recombinase–reduced InSITE enhancer trap lines (*PBac{IT.GAL4.w–}0096*). Although the presence of tandem *attB* and *attP* sites in this vector reduces the rate of transformation, likely through vector suicide via intramolecular recombination, we obtained integrants in both cases using standard injection procedures and verified them by PCR. The insertion into *attP2* drove the expected *ortc2* expression pattern[34] (data not shown). Such enhancer fusions are fully compatible with the InSITE system.

InSITE genetic donor lines and plasmids

We made a collection of *attB*-containing genetic donor lines and injectable donor plasmids (**Supplementary Fig. 1**). All of the reagents described here are publicly available (Online Methods). We established transgenic donor lines, referred to as *P{ID.X}* (*X* is the inserted effector gene and *ID* denotes InSITE donor), for the *GAL80* repressor[17], the *GAL4DBD, GAL4AD* and *VP16AD* split-*GAL4* hemi-drivers[16] as well as the *LexA* and *QF* transcriptional activators[10,11] (**Supplementary Fig. 4**). Taken together, this collection of donor constructs is a versatile toolkit for manipulating gene expression.

Enhancer trap lines are genetically swappable

To test the efficiency of the conversion procedure, we crossed four enhancer trap lines (*PBac{IT.GAL4}1.1*, *PBac{IT.GAL4}3.1*, *PBac{IT.GAL4}5.1* and *PBac{IT.GAL4}6.1*) to Cre recombinase–expressing flies to remove the *loxP*-flanked *mini-white* marker[32]. We identified deletions by loss of *mini-white* expression and confirmed them by PCR (**Fig. 2a**,**b**). This step of the conversion procedure was highly efficient as we recovered no *white*$^+$ flies after treatment with Cre recombinase. Using an *eyeless-FLP* transgene (*eyFLP2*), which expresses Flp recombinase in the eyes, we also confirmed that the donor molecules were readily excised by Flp recombinase, as detected by the loss of *mini-white* expression[35] (**Fig. 2c**).

Next, we crossed eight donor lines, representing all six effectors, to one or more of three different recipient lines, *PBac{IT.GAL4.w–}3.1*, *PBac{IT.GAL4.w–}5.1* and *PBac{IT.GAL4.w–}6.1* in flies that also carried a heat shock–inducible Flp recombinase gene

Table 1 | Efficiency of InSITE genetic swap procedure

Recipient	Donor (line number)	Number of crosses	Crosses with w^+ flies (percentage)	Number tested by PCR	True integrations (percentage)	Recovered swap
PBac{IT.GAL4.w–}6.1	*P{ID.VP16AD}D33.1*	26	9 (34.6%)	9	7 (77.8%)	Yes
PBac{IT.GAL4.w–}3.1	*P{ID.VP16AD}D33.1*	39	9 (23.1%)	8	1 (12.5%)	Yes
PBac{IT.GAL4.w–}6.1	*P{ID.VP16AD}D37.1*	34	8 (23.5%)	No data	No data	Yes
PBac{IT.GAL4.w–}3.1	*P{ID.VP16AD}D37.1*	30	7 (23.3%)	7	0	No
PBac{IT.GAL4.w–}6.1	*P{ID.GAL4DBD}F32.1*	30	5 (16.7%)	5	3 (60%)	Yes
PBac{IT.GAL4.w–}3.1	*P{ID.GAL4DBD}F32.1*	30	10 (33.3%)	9	4 (44.4%)	Yes
PBac{IT.GAL4.w–}6.1	*P{ID.GAL80}E17.1*	29	10 (34.5%)	No data	No data	Yes
PBac{IT.GAL4.w–}3.1	*P{ID.GAL80}E17.1*	30	17 (56.7%)	No data	No data	Yes
PBac{IT.GAL4.w–}6.1	*P{ID.QF}Q10B*	20	4 (20%)	4	3 (75%)	Yes
PBac{IT.GAL4.w–}3.1	*P{ID.QF}Q12A*	18	5 (27.8%)	5	3 (60%)	Yes
PBac{IT.GAL4.w–}5.1	*P{ID.LexA}L34.2L*	19	6 (31.6%)	6	6 (100%)	Yes
PBac{IT.GAL4.w–}5.1	*P{ID.GAL4AD}G12.1*	19	5 (26.3%)	5	3 (60%)	Yes
Total		324	95 (29.3%)	58	30 (51.7%)	12 of 13

At least one line, chosen at random, for each of the six genetic donor elements was tested for the ability to excise and reintegrate into an attP-containing recipient site. Three different enhancer trap target lines were tested. Rates of eyFLP2-resistant white+ flies and true integration events, as assayed by PCR, are shown.

and expressed ΦC31 integrase in the germline[19] (**Supplementary Fig. 5**). We heat-shocked larvae to liberate the circular donor molecule and crossed the resulting flies to flies carrying *eyFLP2* (ref. 35) (**Fig. 2d**,**e**). The presence of *eyFLP2* in the following generation ensured that flies in which the *FRT*-flanked donor cassette had not been excised were not scored as false positives. For all 13 recipient-donor pairs tested, we recovered many *white*$^+$ putative genetic swap flies (16.7–56.6% of crosses giving at least one *white*$^+$ progeny; **Table 1** and **Fig. 2f**).

We selected several putative genetic swaps for molecular and functional validation. For 12 of 13 recipient-donor pairs, by PCR analysis we identified successful genetic swaps (**Fig. 2a**), referred to as *PBac{IS.X.GAL4}* (*X* is the swapped effector gene, and *IS* denotes InSITE swap). For one of the recipient-donor pairs, we recovered only aberrant events. In addition to having the PCR products diagnostic for the new junctions created by integration of the genetic donor constructs, the swaps resulted in a loss of PCR products specific to the intact donor transposon (**Fig. 2a**). Sequencing of the junction between the *mini-white* and *GAL4* genes revealed that, as expected, a single *FRT* site from the genomic donor element was retained between the *loxP* and *attL* sites in the integrated constructs (**Fig. 2g**). To complete the swap, we treated these lines with Cre recombinase and confirmed removal of *GAL4* and *mini-white* by PCR (**Fig. 2a**). We refer to the final, reduced constructs as *PBac{IS.X.w–}*.

In addition to verifying the genetic swap lines, we microinjected a set of *attB*-containing donor plasmids, along with a ΦC31 integrase helper plasmid, into embryos of one of the three InSITE enhancer trap lines (**Supplementary Fig. 3**). For all injections we obtained *white*$^+$ integrants, with integration frequencies between 9.5% and 22.0%, and confirmed the integration of all five donor plasmids by PCR. Finally, we treated the integrants with Cre recombinase to remove *GAL4* and *mini-white*, and confirmed the final conversion products by PCR.

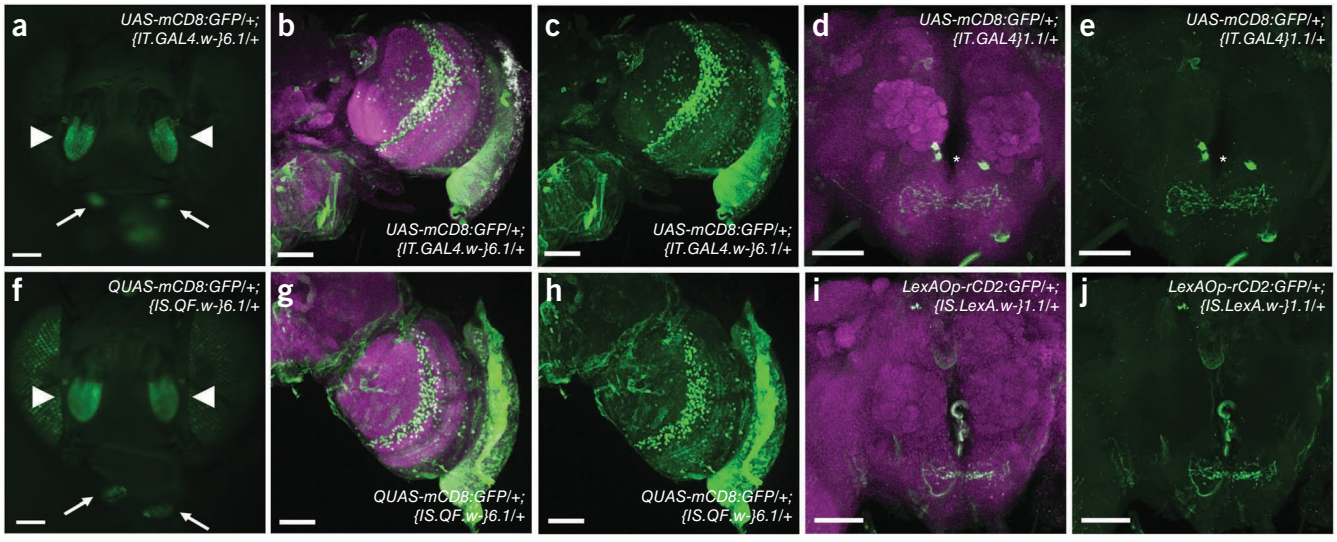

Figure 3 | Functional validation of the *QF* and *LexA* enhancer trap swaps. (**a**–**c**) Expression of the *PBac{IT.GAL4.w–}6.1* enhancer trap. (**d**,**e**) Expression of the *PBac{IT.GAL4}1.1* enhancer trap. (**f**,**h**) Expression of the *PBac{IS.QF.w–}6.1* swap. (**i**,**j**) Expression of the *PBac{IS.LexA.w–}1.1* swap. GFP fluorescence (**a**,**f**) in adult antennae (arrowheads) and maxillary palps (arrows). Adult brains immunostained with anti-mCD8 (green) and anti-Bruchpilot (magenta) (**b**,**g**) or with anti-GFP (green) and anti-Bruchpilot (magenta) (**d**,**i**). mCD8 (green) channel only for images in **b** and **g** is shown in **c** and **h**, and GFP (green) channel only for images in **d** and **i** is shown in **e** and **j**. Asterisks denote a group of cells in which GFP expression was observed in *PBac{IT.GAL4}1.1* but not in the *PBac{IS.LexA.w–}1.1* swap. Scale bars, 100 μm (**a**,**f**), 50 μm (**b**–**e**,**g**–**j**).

Avoiding genetic swap aberrant events

Typically, all integrants into a single *attP* landing site have similar eye colors[36] (**Supplementary Fig. 6**). But we observed aberrant events with different eye colors for many of the above genetic-swap crosses (**Table 1**). Most of these events retained the original donor transposon, but one *FRT* site was inactivated (**Supplementary Fig. 7**). Additionally, we recovered one reciprocal translocation, in which the recipient *attP* site and the donor *attB* site were directly fused (**Supplementary Fig. 7**). Such events have been described previously with ΦC31 integrase–mediated recombination in human cell lines[37]. By selecting appropriate recipient and donor pairs, and following specific markers in the crosses (Online Methods), however, aberrant events can be essentially eliminated.

Functional validation of the enhancer trap swaps

To determine whether the swapped enhancer trap lines were functional, we crossed several Cre recombinase–reduced swaps to appropriate reporters. First, we tested swaps to *QF* and *LexA*. In *PBac{IT.GAL4.w–}6.1* flies, we observed expression in the antennae and maxillary palps and widely in the adult brain (**Fig. 3a–c**).

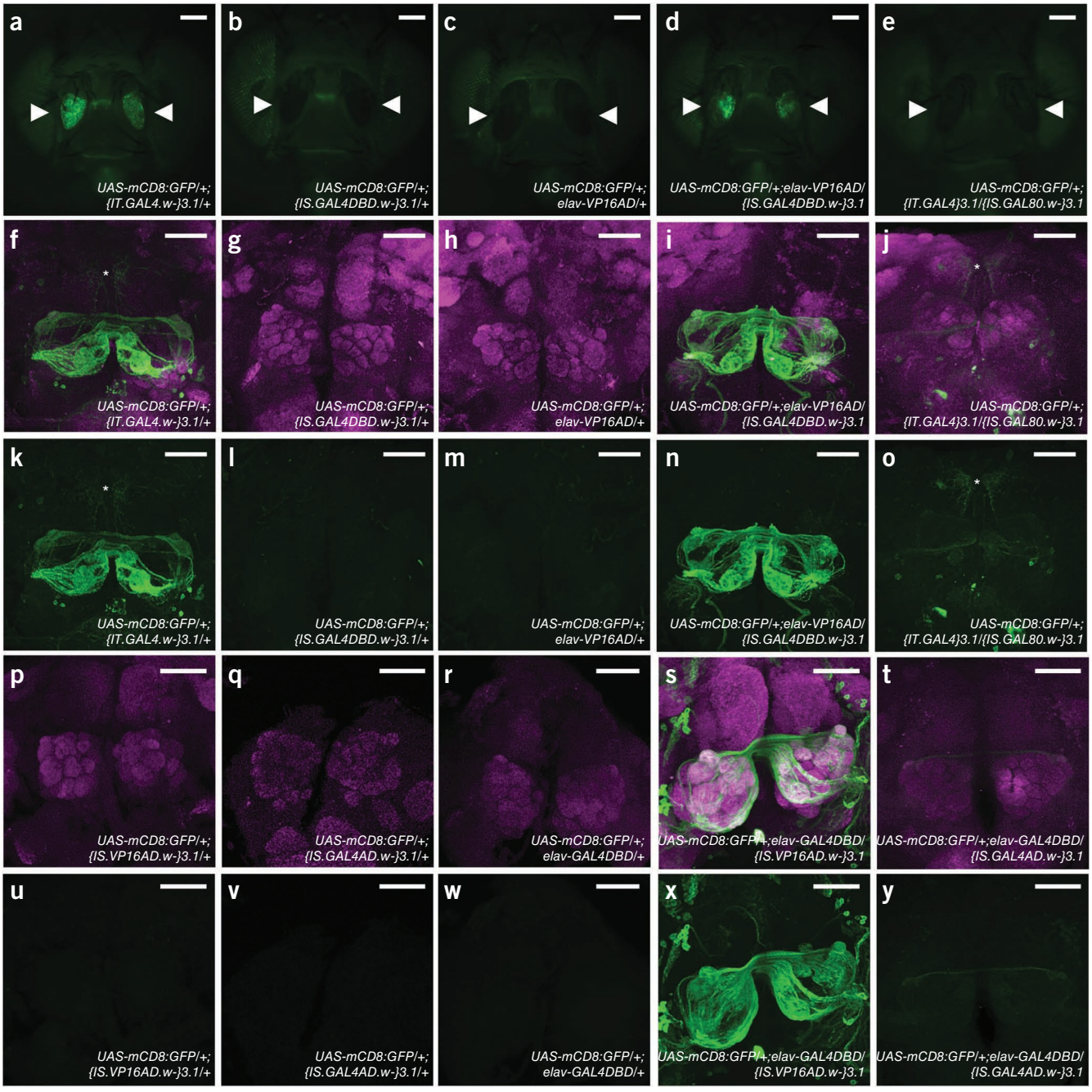

Figure 4 | Functional validation of the split-*GAL4* and *GAL80* enhancer trap swaps. (**a–e**) GFP expression in the antennae (arrowheads) of adult flies of the indicated lines. (**f–j**) Adult brains immunostained with anti-mCD8 (green) and anti-Bruchpilot (magenta). (**k–o**) mCD8 (green) channel only of images in **f–j**. (**p–t**) Adult brains immunostained with anti-mCD8 (green) and anti-Bruchpilot (magenta). (**u–y**) mCD8 (green) channel only of images in **p–t**. Asterisks denote a small number of central brain neurons not targeted by the split-*GAL4* or GAL80 swaps. Scale bars, 100 μm (**a–e**) and 50 μm (**f–y**).

The *PBac{IT.GAL4}1.1* enhancer trap drove expression in a group of neurons in the subesophageal ganglion (**Fig. 3d**,**e**) as well as several neurons in the central brain. In *PBac{IS.QF.w–}6.1*, expression of *QUAS-mCD8:GFP* recapitulated the pattern seen with the UAS-driven expression of *PBac{IT.GAL4.w–}6.1* (**Fig. 3f–h**). In *PBac{IS.LexA.w–}1.1* flies, we detected expression from *LexAOp-rCD2:GFP* in the subesophageal ganglion but not in the central brain neurons (**Fig. 3i**,**j**). Thus the *PBac{IS.LexA.w–}1.1* swap recapitulated some, but not all, features of the original *GAL4* expression pattern.

Next, we tested the conversion to split-*GAL4* hemi-drivers and *GAL80*. We generated swaps of *PBac{IT.GAL4.w–}3.1* to the *GAL4DBD*, *VP16AD* and *GAL4AD* hemi-drivers and *GAL80* and assayed expression of these lines in the antennae and antennal lobes (**Fig. 4**). In *PBac{IT.GAL4.w–}3.1*, we observed expression in the antennae of adult flies (**Fig. 4a**), in several olfactory glomeruli (**Fig. 4f**,**k**) and in several central brain neurons. As expected, both *PBac{IS.GAL4DBD.w–}3.1* and *elav-VP16AD*[16] could not drive *UAS-mCD8:GFP* expression on their own (**Fig. 4b**,**c**,**g**,**h**,**l**,**m**). But, *PBac{IS.GAL4DBD.w–}3.1/elav-VP16AD* drove robust expression in a pattern similar to that in the original *GAL4* line (**Fig. 4d**,**i**,**n** and **Supplementary Table 1**). As with *PBac{IS.LexA.w–}1.1*, we detected a minor difference between the two patterns, with no expression seen in the small number of central brain neurons in the *PBac{IS.GAL4DBD.w–}3.1/elav-VP16AD* brains (**Fig. 4f**,**i**,**k**,**n**).

Neither of the activation domain hemi-driver lines drove *UAS-mCD8:GFP* expression on its own nor did *elav-GAL4DBD*[16] (**Fig. 4p–r**,**u–w**). *PBac{IS.VP16AD.w–}3.1/elav-GAL4DBD* drove expression in a pattern that was similar to but somewhat broader than that in the original *PBac{IT.GAL4}3.1*, whereas *PBac{IS.GAL4AD.w–}3.1/elav-GAL4DBD* drove weak expression in a subset of the glomeruli detected in the parent *GAL4* line (**Fig. 4s**,**t**,**x**,**y** and **Supplementary Table 1**). Such differences are consistent with previous reports that the *VP16AD* hemi-driver is a stronger transcriptional activator than *GAL4AD*[16,38]. Similarly, the *PBac{IS.VP16AD.w–}3.1–PBac{IS.GAL4DBD.w–}3.1* pair drove expression in an essentially identical set of glomeruli as the parent *GAL4* line, whereas *PBac{IS.GAL4AD.w–}3.1–PBac{IS.GAL4DBD.w–}3.1* was expressed weakly in an overlapping but restricted subset of glomeruli (**Supplementary Table 1**). Likewise, *PBac{IS.VP16AD.w–}6.1* in combination with *elav-GAL4DBD* largely recapitulated the original expression pattern seen for *PBac{IT.GAL4}6.1* (**Supplementary Fig. 8**).

As expected, *PBac{IS.GAL80.w–}3.1* eliminated most expression driven by the original *PBac{IT.GAL4}3.1* line (**Fig. 4e**,**j**,**o**). Similar to the split-*GAL4* lines, *GAL80* did not target the small group of central brain neurons (**Fig. 4f**,**j**,**k**,**o**), suggesting that this expression was influenced by sequences inside *GAL4* itself.

For most of the swaps, the resultant expression was strongly predicted by the original *GAL4* pattern. In 3 of 10 cases, the expression patterns overlapped with the original pattern but also displayed substantial differences. Expression of *PBac{IS.QF.w–}3.1* was similar to that in the original *PBac{IT.GAL4.w–}3.1* line in the antennae and olfactory glomeruli, but we observed new expression in a single glial subtype (cortex glia)[39] and in trachea (**Supplementary Fig. 8** and **Supplementary Table 1**). In a second case, for *PBac{IS.GAL4DBD.w–}6.1*, the pattern of expression overlapped with that for *PBac{IT.GAL4}6.1* in both the antennae and the adult brain but was much sparser and was not detected in the maxillary palps. Finally, *PBac{IS.GAL80.w–}6.1* repression of *PBac{IT.GAL4}6.1* was incomplete (**Supplementary Fig. 8**). In this case, as *GAL4* and *GAL80* are presumably being expressed at similar levels, it is not clear that complete repression would be expected.

DISCUSSION

We demonstrated that InSITE enhancer traps can be efficiently swapped and made to express a split-*GAL4* hemi-driver, *GAL80*, *LexA* or *QF*. This will allow lines with overlapping expression patterns to be used in an intersectional manner to target restricted subsets of the original patterns. Using this system, it should be possible to generate highly specific driver lines targeting small populations of cells or tissues. This will be useful in many developmental and cell-biological experiments, allowing the tissue-specific requirements of genes to be mapped with high precision and the dissection of neural circuits at the level of single neuron types.

One advantage of the InSITE system is that the effector swap can be done genetically, through a series of crosses, bypassing the labor-intensive step of DNA microinjection. Whereas other approaches exist for repurposing enhancer expression patterns, such as constructed enhancer fusions, these strategies have previously required that new constructs must be cloned and transformed for each new desired fusion[4]. The InSITE-compatible enhancer fusion vector we describe allows one to make a single *GAL4* construct and then swap it for any of the available donor lines *in vivo*. In addition, the InSITE genetic swap approach is easily scalable, making it possible to simultaneously exchange large numbers of lines with multiple donor constructs.

The majority of the swaps captured most features of the original *GAL4* expression patterns. In some cases, however, either prominent features of the *GAL4* pattern were lost or we observed new expression patterns. These changes may have resulted from differences in the strength or responsiveness of reporter lines. Alternately, the swap may have modified some combination of enhancer spacing and sequence composition flanking the promoter. As the InSITE donors are essentially identical outside the effector sequence, these effects are likely intrinsic properties of the effector sequence itself. Therefore, any approach using these effectors would also likely be subject to such context-specific cryptic regulatory activities. These occasional discrepancies between the original and swapped patterns underscore the importance of having a versatile, high-throughput system that allows many orthogonal intersectional strategies to be quickly tested in parallel.

The modular nature of the InSITE platform makes this system forward-compatible. Recent work has described refinements to the existing binary systems[13,24,38]. Such new reagents and many unanticipated future technologies can be readily incorporated into the InSITE system and will be useful in designing additional intersectional strategies.

Although we focused primarily on binary system expression and the refinement of expression patterns, many additional elaborations of this system are possible because of the fact that *GAL4* can be replaced with any other sequence. For instance, it is possible to design strategies to mutate or modify loci near the transposon insertion site. In particular, because the genetic swap leaves behind a single *FRT* site, it is possible to use genetic swap lines together with other *FRT*-containing transposons (such as the Exelixis and Drosdel collections) to make deletions[31].

These deletions, which could disrupt nearby genes and regulatory elements, can be designed to leave behind either *GAL4* or the swapped effector. This provides another approach to segment complex expression patterns, by altering the surrounding regulatory elements. Thus, the InSITE system is a versatile toolkit both for capturing and manipulating gene activity. As the methods described here use recombinases that work in other model organisms, this system should be easily adaptable.

METHODS

Methods and any associated references are available in the online version of the paper at http://www.nature.com/naturemethods/.

Accession codes. InSITE-compatible enhancer fusion vector pBMPGal4LWL, HQ888842; injectable donor plasmid pBPHLWL, HQ888843; genetic donor transposon plasmid pXN-FBLWLF, HQ888844; *piggyBac* enhancer trap plasmid pXL-BACII-attPGAL4LwL, HQ888845; and *P* element enhancer trap plasmid pXN-attPGal4LwL, HQ888846.

Note: Supplementary information is available on the Nature Methods website.

ACKNOWLEDGMENTS

We thank members of the Clandinin laboratory for helpful advice; M. Müller (University of Basel), M. Wernet (Stanford University), T. Schwabe (Stanford University), G. Dietzl (Stanford University), J. Bateman (Bowdoin College), L. Luo (Stanford University), C.-H. Lee (US National Institutes of Health) and P. Schedl (Princeton University) for reagents; S. Burns for assistance with experiments; and A. Parks at the Bloomington *Drosophila* Stock Center. M. Klovstad, L. Luo and T. Schwabe provided valuable comments on the manuscript. M. Spletter helped score antennal lobes. This work was funded by a National Institutes of Health Director's Pioneer Award DP1 OD003530 (T.R.C.) and by National Institutes of Health R01 EY015231 (T.R.C.). D.M.G. and M.A.S. were supported by Stanford Dean's Postdoctoral fellowships.

AUTHOR CONTRIBUTIONS

D.M.G. and T.R.C. designed the experiments; D.M.G., M.A.S., X.J.G., F.J.L., C.-C.L., C.J.P. and T.R.C. performed the experiments; S.B. provided critical reagents; and D.M.G. and T.R.C. wrote the manuscript.

COMPETING FINANCIAL INTERESTS

The authors declare no competing financial interests.

Published online at http://www.nature.com/naturemethods/.
Reprints and permissions information is available online at http://npg.nature.com/reprintsandpermissions/.

1. Brand, A.H. & Perrimon, N. Targeted gene expression as a means of altering cell fates and generating dominant phenotypes. *Development* **118**, 401–415 (1993).
2. O'Kane, C.J. & Gehring, W.J. Detection in situ of genomic regulatory elements in *Drosophila*. *Proc. Natl. Acad. Sci. USA* **84**, 9123–9127 (1987).
3. Ejsmont, R.K., Sarov, M., Winkler, S., Lipinski, K.A. & Tomancak, P. A toolkit for high-throughput, cross-species gene engineering in *Drosophila*. *Nat. Methods* **6**, 435–437 (2009).
4. Pfeiffer, B.D. *et al.* Tools for neuroanatomy and neurogenetics in *Drosophila*. *Proc. Natl. Acad. Sci. USA* **105**, 9715–9720 (2008).
5. Venken, K.J. *et al.* Versatile P[acman] BAC libraries for transgenesis studies in *Drosophila melanogaster*. *Nat. Methods* **6**, 431–434 (2009).
6. Luo, L., Callaway, E.M. & Svoboda, K. Genetic dissection of neural circuits. *Neuron* **57**, 634–660 (2008).
7. Korzh, V. Transposons as tools for enhancer trap screens in vertebrates. *Genome Biol.* **8** (Suppl. 1), S8 (2007).
8. Stanford, W.L., Cohn, J.B. & Cordes, S.P. Gene-trap mutagenesis: past, present and beyond. *Nat. Rev. Genet.* **2**, 756–768 (2001).
9. Bellen, H.J. Ten years of enhancer detection: lessons from the fly. *Plant Cell* **11**, 2271–2281 (1999).
10. Lai, S.L. & Lee, T. Genetic mosaic with dual binary transcriptional systems in *Drosophila*. *Nat. Neurosci.* **9**, 703–709 (2006).
11. Potter, C.J., Tasic, B., Russler, E.V., Liang, L. & Luo, L. The Q system: a repressible binary system for transgene expression, lineage tracing, and mosaic analysis. *Cell* **141**, 536–548 (2010).
12. Suster, M.L., Seugnet, L., Bate, M. & Sokolowski, M.B. Refining GAL4-driven transgene expression in *Drosophila* with a GAL80 enhancer-trap. *Genesis* **39**, 240–245 (2004).
13. Bohm, R.A. *et al.* A genetic mosaic approach for neural circuit mapping in *Drosophila*. *Proc. Natl. Acad. Sci. USA* **107**, 16378–16383 (2010).
14. Stockinger, P., Kvitsiani, D., Rotkopf, S., Tirian, L. & Dickson, B.J. Neural circuitry that governs *Drosophila* male courtship behavior. *Cell* **121**, 795–807 (2005).
15. Gordon, M.D. & Scott, K. Motor control in a *Drosophila* taste circuit. *Neuron* **61**, 373–384 (2009).
16. Luan, H., Peabody, N.C., Vinson, C.R. & White, B.H. Refined spatial manipulation of neuronal function by combinatorial restriction of transgene expression. *Neuron* **52**, 425–436 (2006).
17. Lee, T. & Luo, L. Mosaic analysis with a repressible cell marker for studies of gene function in neuronal morphogenesis. *Neuron* **22**, 451–461 (1999).
18. Bateman, J.R., Lee, A.M. & Wu, C.T. Site-specific transformation of *Drosophila* via phiC31 integrase-mediated cassette exchange. *Genetics* **173**, 769–777 (2006).
19. Bischof, J., Maeda, R.K., Hediger, M., Karch, F. & Basler, K. An optimized transgenesis system for *Drosophila* using germ-line-specific phiC31 integrases. *Proc. Natl. Acad. Sci. USA* **104**, 3312–3317 (2007).
20. Golic, M.M., Rong, Y.S., Petersen, R.B., Lindquist, S.L. & Golic, K.G. FLP-mediated DNA mobilization to specific target sites in *Drosophila* chromosomes. *Nucleic Acids Res.* **25**, 3665–3671 (1997).
21. Horn, C. & Handler, A.M. Site-specific genomic targeting in *Drosophila*. *Proc. Natl. Acad. Sci. USA* **102**, 12483–12488 (2005).
22. Oberstein, A., Pare, A., Kaplan, L. & Small, S. Site-specific transgenesis by Cre-mediated recombination in *Drosophila*. *Nat. Methods* **2**, 583–585 (2005).
23. Schlake, T. & Bode, J. Use of mutated FLP recognition target (FRT) sites for the exchange of expression cassettes at defined chromosomal loci. *Biochemistry* **33**, 12746–12751 (1994).
24. Yagi, R., Mayer, F. & Basler, K. Refined LexA transactivators and their use in combination with the *Drosophila* Gal4 system. *Proc. Natl. Acad. Sci. USA* **107**, 16166–16171 (2010).
25. Groth, A.C., Fish, M., Nusse, R. & Calos, M.P. Construction of transgenic *Drosophila* by using the site-specific integrase from phage phiC31. *Genetics* **166**, 1775–1782 (2004).
26. Thorpe, H.M. & Smith, M.C. *In vitro* site-specific integration of bacteriophage DNA catalyzed by a recombinase of the resolvase/invertase family. *Proc. Natl. Acad. Sci. USA* **95**, 5505–5510 (1998).
27. Woltjen, K. *et al.* piggyBac transposition reprograms fibroblasts to induced pluripotent stem cells. *Nature* **458**, 766–770 (2009).
28. Horn, C., Offen, N., Nystedt, S., Hacker, U. & Wimmer, E.A. piggyBac-based insertional mutagenesis and enhancer detection as a tool for functional insect genomics. *Genetics* **163**, 647–661 (2003).
29. Rad, R. *et al.* PiggyBac transposon mutagenesis: a tool for cancer gene discovery in mice. *Science* **330**, 1104–1107 (2010).
30. Li, X. *et al.* piggyBac internal sequences are necessary for efficient transformation of target genomes. *Insect Mol. Biol.* **14**, 17–30 (2005).
31. Thibault, S.T. *et al.* A complementary transposon tool kit for *Drosophila melanogaster* using P and piggyBac. *Nat. Genet.* **36**, 283–287 (2004).
32. Siegal, M.L. & Hartl, D.L. Transgene coplacement and high efficiency site-specific recombination with the Cre/loxP system in *Drosophila*. *Genetics* **144**, 715–726 (1996).
33. Maggert, K.A., Gong, W.J. & Golic, K.G. Methods for homologous recombination in *Drosophila*. *Methods Mol. Biol.* **420**, 155–174 (2008).
34. Gao, S. *et al.* The neural substrate of spectral preference in *Drosophila*. *Neuron* **60**, 328–342 (2008).
35. Newsome, T.P., Asling, B. & Dickson, B.J. Analysis of *Drosophila* photoreceptor axon guidance in eye-specific mosaics. *Development* **127**, 851–860 (2000).
36. Venken, K.J., He, Y., Hoskins, R.A. & Bellen, H.J. P[acman]: a BAC transgenic platform for targeted insertion of large DNA fragments in *D. melanogaster*. *Science* **314**, 1747–1751 (2006).
37. Malla, S., Dafhnis-Calas, F., Brookfield, J.F., Smith, M.C. & Brown, W.R. Rearranging the centromere of the human Y chromosome with phiC31 integrase. *Nucleic Acids Res.* **33**, 6101–6113 (2005).
38. Pfeiffer, B.D. *et al.* Refinement of tools for targeted gene expression in *Drosophila*. *Genetics* **186**, 735–755 (2010).
39. Awasaki, T., Lai, S.L., Ito, K. & Lee, T. Organization and postembryonic development of glial cells in the adult central brain of *Drosophila*. *J. Neurosci.* **28**, 13742–13753 (2008).

ONLINE METHODS

Cloning enhancer-trap transposons. For pXL-BacII-attP-Gal4LWL, first, the *attP* site was excised from pUASTP2 (ref. 18) (obtained from J. Bateman, Bowdoin College) with EcoRI and ligated into the EcoRI site of pBluescript, to make pBS-attP. Next, a linker fragment, *SPpolyF/R*, was made by annealing and phosphorylating the SPpolyF and PSpolyR oligos (all oligos were obtained from Integrated DNA Technologies; see **Supplementary Table 2** for oligo sequences) and this linker was ligated into PstI and SacI cut pBS-attP, destroying the SacI site, to make pBS-attPΔS3. A second linker fragment, HKpolyF/R, was made with the HKpolyF and KHpolyR oligos. pBS-attPΔS3 was cut with HindIII and KpnI, and the *HKpolyF/R* linker was inserted to generate pBS-attPΔS^{+}S1.

Next, a fragment containing the *P* promoter was amplified from pLAPVPRA (D.M.G. and M. Müller, unpublished data) using the pPromF and pPromR primers (see **Supplementary Table 3** for sequences of PCR and sequencing primers). The *P* promoter fragment was cloned into pCRII-TOPO (Invitrogen), to generate pCRII-Pprom1-2. This vector and pBS-attPΔS^{+}S1 were both digested sequentially with BamHI and HindIII, and the *P* promoter fragment was cloned into pBS-attPΔS^{+}S1 to make pBS-attPΔS^{+}SPprom1. This vector was cut with BamHI and SacI. A BamHI and SacI fragment containing *GAL4* and the *hsp70* 3′ untranslated region (UTR) was isolated from pGaTB[1] (obtained from M. Wernet, Stanford University) and ligated into pBS-attPΔS^{+}SPprom1 to generate pBS-attPPpromGal4.

In parallel, the *mini-white* gene was obtained as an EcoRI fragment from pC4YM[40] (from M. Müller, University of Basel) and ligated between two *loxP* sites into the EcoRI site of pBLLΔ (from M. Müller[40]) to make pBLLΔ-miniwhite1. A NotI, BamHI fragment containing *mini-white* flanked by *loxP* sites was isolated and cloned into the NotI, BamHI sites of pXL-BacII-ECFP[30,41] (obtained from L. Luo, Stanford University) to make pXL-BacII-lox-miniwhite-lox. Finally, to make pXL-BacII-attPGal4LWL, a NotI fragment containing *attP-Pprom-GAL4-hsp70* 3′ UTR was isolated from pBS-attPPpromGal4 and ligated into the NotI site of pXL-BacII-lox-miniwhite-lox. The correct insert orientation was determined by diagnostic digests and by sequencing with primers pPromF, pPromR, MW300Up and 9-1.

For pXN-attPGal4LWL, a KpnI, BamHI fragment from pXL-BacII-attPGal4LWL was ligated into the KpnI, BamHI sites of pXN[42] (from P. Schedl, Princeton University), between the *P* element ends. This vector was recut with NotI and BamHI, and a NotI, BamHI fragment containing *mini-white* flanked by *loxP* sites was inserted to make pXN-LWL. pXN-LWL was then cut with NotI and was ligated to the NotI fragment containing *attP-Pprom-GAL4-hsp70* 3′ UTR isolated from pBS-attPPpromGal4 to make pXN-attPGal4LWL. The correct orientation of the insert was confirmed by diagnostic digests and sequencing with the P5′inF and MW5′R primers.

Cloning injectable donor plasmids. For pBPHLWL, two pairs of oligos that encoded a multiple cloning site with the restriction sites KpnI-HindIII-BamHI-NotI-MluI-AscI-XbaI-ClaI-NheI-PacI-SphI-SpeI-BglII-SacI were annealed and phosphorylated to make Oligo1F/R and Oligo2F/R. Next, pBluescriptKSII^{+} was cut with KpnI and XbaI and Oligo1F/R was inserted to generate pBS-Oligo1. pBS-Oligo1 was cut with XbaI and SacI, and Oligo2F/R was ligated into this backbone to make pBSO1O2. Next, a ClaI, SpeI fragment containing the *hsp70* 3′ UTR was isolated from pGaTB and cloned into the ClaI, SpeI sites of pBSO1O2. The resulting vector was cut with SpeI and BglII, and was ligated to an XbaI, BamHI fragment containing *loxP-mini-white-loxP* from pBLLΔ-miniwhite1, generating the plasmid pBSO1O2hsp70LWL.

In parallel, the *attB* site from piB-GFP[18] (obtained from J. Bateman) was isolated as a KpnI, HindIII fragment and cloned into pBluescriptKSII+ to make pBS-attB. A HindIII, BamHI fragment containing the *P* minimal promoter (from pCRII-Pprom1-2) was ligated into the HindIII, BamHI sites of pBS-attB, to make pBS-attBPprom.

Finally, a KpnI, BamHI fragment containing *attB* and the minimal P promoter was isolated from pBS-attBPprom and ligated into the KpnI, BamHI sites of pBSO1O2hsp70LWL to generate the pBPHLWL donor plasmid. pBPHLWL was sequenced with primers M13For, M13Rev, hsp3′F, MW5′R, MW3′F, hsp3′R(seq), PpromF(seq), MW5′F(seq), MW2F(seq), MW2R(seq), MW3F(seq), MW3R(seq), MW4F(seq), MW4R(seq), MW6F(seq) and MW6R(seq).

For pBPHLWL-Gal80, a NotI, XbaI fragment containing *GAL80* from pCASPTubGAL80 (ref. 17) (obtained from T. Schwabe, Stanford University), was cloned into the NotI, XbaI sites of pBPHLWL. The insert was verified by sequencing using primers PpromF(seq), MW5′R, Gal80F1(seq) and Gal80R1(seq).

For pBPHLWL-Gal4AD, a NotI, AscI fragment containing the *GAL4AD*-leucine zipper fusion from pActPL-Gal4AD[16] (obtained from Addgene) was inserted in the MCS of pBPHLWL and verified by sequencing with the PpromF(seq) and MW5′R primers.

For pBPHLWL-VP16AD, a NotI, AscI fragment containing the *VP16AD*-leucine zipper fusion from pActPL-VP16AD[16] (obtained from Addgene) was inserted in the MCS of pBPHLWL and verified by sequencing with the PpromF(seq) and MW5′R primers.

For pBPHLWL-Gal4DBD, a NotI, AscI fragment containing the *GAL4DBD*-leucine zipper fusion from pActPL-Gal4DBD[16] (obtained from Addgene) was inserted in the MCS of pBPHLWL and verified by sequencing with the PpromF(seq) and MW5′R primers.

For pBPHLWL-LexA, a NotI, XbaI fragment containing *LexA* from pGD319 (obtained from G. Dietzl, Stanford University) was cloned into the MCS of pBPHLWL and verified by sequencing with primers PpromF(seq), MW5′R, LexA1F and LexA1R.

For pBPHLWL-QF, a BamHI and SpeI fragment containing *QF*[11] from pXN-FBLWLF-QF was ligated into the BamHI, XbaI sites of pBPHLWL and verified by sequencing with the PpromF(seq) and MW5′R primers.

Cloning genetic donor transposons. For pXN-FBLWLF, two sets of *FRT* site–containing oligos were used to make *5′FRT(KpnI)F/R* and *3′FRT(Not-Sac)F/R*. Next, pBS-attBPprom was cut with KpnI and *5′FRT(KpnI)F/R* was inserted to generate the plasmid pBSattBPprom^{+}5′FRT5, which had a tandem insertion of the oligo. The orientation of the insert was verified by sequencing with M13For. To reduce this tandem insert, pBSattBPprom^{+}5′FRT5 was cut with AscI, gel purified and religated to generate pBSFattBPprom. This plasmid was then cut with NotI and SacI, and *3′FRT(Not-Sac)F/R* was inserted to make pBSFattBPpromF. Next, a KpnI, XhoI FattBPpromF fragment from pBSFattBPpromF was

doi:10.1038/nmeth.1561

ligated into the KpnI, SalI sites of the pXN vector to make pXN-FattBPpromF2-1. A linker containing specific restriction sites (NotI-EcoRV-PacI-SphI-AvrII-NheI-MluI-BglII) was made from a pair of oligos (GCNotI F (dXho) and GCNotI R (dXho)) and ligated into the NotI site of pXN-FattBPpromF2-1. This plasmid was cut with BglII and NheI, and an XbaI, BamHI *loxP-mini-white-loxP* from pBLLΔ-miniwhite1 was inserted to make pXN-FBLWLF. pXN-FBLWLF was confirmed by sequencing with the P5′inF and MW5′R primers.

For pXN-FBLWLF-Gal80, a BamHI, SphI fragment containing *GAL80* and the *hsp70* 3′ UTR from pBPHLWL-Gal80 was cloned into the MCS of pXN-FBLWLF and confirmed by diagnostic digests and sequencing with the P5′inF primer.

For pXN-FBLWLF-GAL4AD, a BamHI, SphI fragment containing *GAL4AD* and the *hsp70* 3′ UTR from pBPHLWL-GAL4AD was cloned into the MCS of pXN-FBLWLF and confirmed by diagnostic digests and sequencing with the P5′inF primer.

For pXN-FBLWLF-VP16AD, a BamHI, PacI fragment containing *VP16AD* and the *hsp70* 3′ UTR from pBPHLWL-VP16AD was cloned into the MCS of pXN-FBLWLF and confirmed by diagnostic digests and sequencing with the P5′inF primer.

For pXN-FBLWLF-Gal4DBD, a BamHI, PacI fragment containing *GAL4DBD* and the *hsp70* 3′ UTR from pBPHLWL-Gal4DBD was cloned into the MCS of pXN-FBLWLF and confirmed by diagnostic digests and sequencing with the P5′inF and MW5′R primers.

For pXN-FBLWLF-LexA, a NotI, PacI fragment containing *LexA* and the *hsp70* 3′ UTR from pBPHLWL-LexA was cloned into the MCS of pXN-FBLWLF and confirmed by diagnostic digests and sequencing with the P5′inF primer.

For pXN-FBLWLF-QF, using pBac-GH146-QF-hsp70 (ref. 11) as substrate, *QF* and *hsp70* were separately PCR-amplified with a shared sequence (5′-TAAGCACTAGTGCAGATCTTATCGAT AC-3′) between the *QF* and *hsp70* regions. For *QF*, the following primers were used: BHI-QF-FOR/QFREV-hsp70-LNKR. For *hsp70*, the following primers were used: pGaTn-hsp70REV-NotI-BH1/hsp70-FOR-QF-LNKR. The *QF* and *hsp70* PCR products were annealed and the BHI-QF-FOR and pGaTn-hsp70REV-NotI-BH1 primers were used to PCR amplify a BamHI-*QF*-SpeI-BglII-*hsp70*-NotI-BamHI cassette, which was cloned into the BamHI site of pXN-FBLWLF. An insert in the correct orientation was verified by sequencing.

Cloning the enhancer fusion vector. For pBMPGal4LWL, pBSO1O2 was cut with BamHI and BglII, and a BamHI fragment containing *GAL4*, the *hsp70* 3′ UTR and *loxP*-flanked *mini-white* from pXL-BacII-attPGal4LWL was ligated into these sites to make pBSO1O2-Gal4LWL. A correctly oriented insert was cut with NotI, treated with mung bean nuclease and religated to destroy the NotI site. Next, to make a multi-cloning site, a pair of oligos (PstI-SacI EF linker For and PstI-SacI EF linker Rev) were phosphorylated, annealed and ligated into the SacI and PstI sites of pBS-attP. Next, the multicloning site and *attP* site were liberated using HindIII and ligated into the HindIII site of pBPHLWL. An insert with the correct orientation was identified and a fragment containing *attB*, the multi-cloning site, and *attP* was cut out of this plasmid with KpnI and BamHI. Finally, this fragment was ligated into the KpnI, BamHI sites of pBSO1O2-Gal4LWL to make pBMPGal4LWL.

For pBMPGal4LWL-ortc2b, a fragment containing the *ortc2b* regulatory region was amplified from pChs-ATTB-OrtC2-Gal4 (ref. 34) (obtained from C.-H. Lee, National Institutes of Health) using the ortc2b For and ortc2b Rev primers. A NotI site was added to the 5′ end of the PCR product, which was then cloned into pCRII-TOPO (Invitrogen). The *ortc2b* fragment was cut out of pCRII-TOPO with NotI and BamHI and cloned into NotI, BglII cut pBMPGal4LWL.

Fly methods. Flies were grown on molasses food at 22–25 °C. Injections were performed as previously described by Rainbow Transgenic Flies[43]. P element constructs were transformed using a standard Δ2-3 helper plasmid. *PiggyBac* constructs were transformed using the pBSII-hs-orf[30] helper plasmid (obtained from L. Luo, Stanford University). Injected *attB* donor constructs (pBPHLWL derivatives) were transformed using the *ΦC31* integrase helper plasmid pBS130. Flies were obtained from the Bloomington *Drosophila* Stock Center (BDSC) (*y, w; P{CaryP}attP2*) to test the integration of pBMPGal4LWL.

Cre recombinase reductions. To prepare swappable enhancer trap lines for injection of the donor plasmid (or genetic conversion), females containing a convertible enhancer trap line were crossed to males carrying the Cre recombinase (*y, w; MKRS, P{hsFLP}86E/TM6B, P{w[+mC] = CrewDH2, Tb*[1], or *y, w; noc[Sco]/CyO, P{w[+mC] = CrewDH1*, from BDSC). Males containing both the enhancer trap and the Cre recombinase–encoding chromosome were crossed to the appropriate balancer line, and single male progeny were used to establish a balanced *white* minus enhancer trap stock (**Supplementary Fig. 6**). The clean excision of *mini-white* was confirmed by PCR. The same procedure was used to remove the *mini-white* marker and original *GAL4* gene from integrant flies. Excision using Cre recombinase was highly efficient, approaching 100%.

Genetic conversion crosses. To carry out the genetic swap procedure (**Fig. 1b** and **Supplementary Fig. 5**), first a *y, w, hs-FLP, vas-ΦC31* integrase recombinant X chromosome was established. Recombinants were scored for the presence of GFP (marking the *J15*, *vas-ΦC31* integrase transgene[19]) and then tested by PCR for the presence of FLP recombinase (FLP) (using the FLP Set1 Forward/FLP Set1 Reverse and FLP Set2 Forward/FLP Set2 Reverse primers). *y, w, hs-FLP, vas-ΦC31; Recipient(enhancer trap)w-/Balancer* stocks were made, and virgins were crossed to genetic donor males (**Supplementary Fig. 5**). These flies were allowed to lay eggs for 2–4 days, then flipped onto fresh food. The vials containing the progeny of this cross were then heat-shocked in a 37 °C water bath for 1 h, every day, until most of the progeny had pupated. The resulting progeny had eyes which were either completely white, or had small patches of orange or red variegation (**Fig. 2d**,**e**). Heat-shocked *y, w, hs-FLP, vas-ΦC31*; *Donor*/+; *Recipient(w-)*/+ males were crossed to *y, w, eyFLP2*; *Balancer* virgins and *white* plus putative genetic swaps were balanced. Integration of the genetic donor construct in the enhancer trap was confirmed by PCR. To complete the swap, the enhancer trap containing the integrated genetic donor construct was reduced using Cre recombinase. Genetic donor constructs lose *mini-white* expression when crossed to *eyFLP2*, which excises the *FRT*-flanked donor cassette in the eye. At least eight independent lines

were tested for the *VP16AD*, *GAL80*, *GAL4AD, GAL4DBD*, *LexA*, and *QF* constructs, and every line had white eyes in the presence of *eyFLP2* (**Fig. 2c**), with the exception of one *VP16AD* line (*P{ID.VP16AD}39.1D1*), which was pupal lethal with *eyFLP2*.

Maintaining the genetic donor lines together with the *y, w, hs-FLP, vas-ΦC31* chromosome for many generations may lead to degradation of the donor construct.

Avoiding genetic swap aberrant events. As all aberrant events were associated with the original donor site, crosses should be set up with recipient and donor lines on different chromosomes. This way, putative genetic swap lines that do not map to the recipient chromosome can be immediately discarded. In addition, by using recipient and donor lines with distinct eye colors, the level of *mini-white* expression can facilitate the identification of *bona fide* swaps. To avoid reciprocal translocations, recipient and donor lines can be molecularly mapped (**Supplementary Fig. 4**)[44,45] and selected such that any translocations will be lethal (for instance, by generating a dicentric or acentric chromosome). Finally, by selecting *white*$^+$ flies in the final step that also contain the balancer or dominant marker that was opposite the donor chromosome in the previous generation, it is possible to select against aberrant events. In our experience, selecting matched donors and recipients in this way eliminated all aberrant events. Even if no effort was made to select against aberrant events, the frequency of true events among w^+ putative swaps was quite high (averaging 51.7%; **Table 1**).

Functional tests of enhancer trap swaps. The following lines were used to functionally test the split-*GAL4* enhancer trap swaps: *w; P{UAS:2xEGFP}; P{elav-GAL4.DBD}H4A1*, *w; P{UAS:2xEGFP}; P{elav-GAL4.AD}I1A1*, *w; P{UAS:2xEGFP}; P{elav-VP16.AD}G3A1* (from BDSC)[16]. For testing the enhancer trap swaps, the *UAS:2xEGFP* chromosome present in the *elav* split-*GAL4* lines was replaced with *UAS:mCD8-GFP*[17]. *w; LexAop:rCD2-GFP*[10] (obtained from C.-H. Lee) reporter lines were used to monitor LexA-driven gene expression. w; *P{QUAS-mCD8-GFP.P}5J* was used to monitor QF expression[11]. The following injected enhancer trap swap lines were functionally tested: *PBac{IS.VP16AD.w-}6.1(11.1)*, *PBac{IS.GAL80.w-}6.1(39.1)*, *PBac{IS.GAL4AD.w-}3.1(33.1)*, *PBac{IS.GAL4DBD.w-}3.1(51.1)* and *PBac{IS.LexA.w-}1.1 (44.1)*. The following genetic swap lines were functionally tested: *PBac{IS.VP16AD.w-}6.1(D37-6)*, *PBac{IS.GAL80.w-}6.1(E17-30)*, *PBac{IS.GAL4DBD.w-}6.1(F32-2)*, *PBac{IS.GAL80.w-}3.1 (E17-12)*, *PBac{IS.VP16AD.w-}3.1(D33-16)*, *PBac{IS.QF.w-}6.1(Q10B-7)* and *PBac{IS.QF.w-}3.1(Q12A-10)*. GFP expression in adult animals was visualized on a Zeiss M2Bio stereomicroscope and fluorescence images were acquired using a SPOT-RT digital camera (Diagnostic Instruments, Inc.).

Confirming Cre-mediated reductions and injected integration events by PCR. To confirm the deletion of *mini-white* by Cre, the subsequent integration of the microinjected *attB*-containing donor construct and the Cre-mediated reduction of the integrant, a set of diagnostic PCR primers was used (**Fig. 2a**,**b** and **Supplementary Fig. 3**). The following primer pairs were used on the *piggyBac* constructs: MW3′F2/pBAC3′R4, Gal4 3′F2/MW5′R2, pBAC5′F1/attP R1, Gal4 3′F2/pBAC3′R4, pBSF1/attP R1, pBAC5′F1/attB R1 and construct-specific primer/pBAC3′R4. Construct-specific primers: Gal80 3′F1, Gal4AD 3′F1 (note: also works on *VP16AD*), Gal4DBD 3′F1, LexA 3′F1, or QF 3′F1.

To confirm integration into the *P* element constructs (data not shown), the above primer pairs can be used, with two modifications. P5′inF can be used in place of pBAC5′F1, and P3′Rnew2R can be used in place of pBAC3′R4.

Confirming genetic swaps by PCR. The primers that were used to confirm the injection-based enhancer trap swaps were also used to validate the genetic swaps, with one exception. In the genetic swaps, the sequence corresponding to the vector backbone in the injected swaps does not exist, so primer MW3′F2 was substituted for pBSF1 in primer pair number 5. In addition, another set of PCRs using the primer pairs P5′inF/attBR1 (primer pair 8 in **Fig. 2b**) and MW3′F2/ P3′Rnew2R (primer pair 9 in **Fig. 2b**) were done on the genetic swap lines, to confirm the loss of the donor element 5′ and 3′ junctions.

Confirming insertion of the pBMPGal4LWL-ortc2 enhancer fusion vector. To confirm the insertion of pBMPGal4LWL into *P{CaryP}attP2*, the following primers were used: pBSF1/attP R1, yellow 3′F2/attB R1 and yellow 3′F2/ortc2 5′R1.

Splinkerette mapping of transposon insertion sites. Fifteen of the *piggyBac* enhancer trap lines and twenty four genetic donor *P element* lines were mapped using Splinkerettes[44] and localized using Flybase to BLAST search the *Drosophila melanogaster* genome[46]. Line *PBac{IT.GAL4}1.1* was inserted in an intron of the *sarah* (*sra*) gene. Line *PBac{IT.GAL4}3.1* was inserted in an intron of the *desaturase1* (*desat1*) gene. Line *PBac{IT.GAL4}5.1* was inserted within a microRNA cluster in *mir-2498*. Line *PBac{IT.GAL4}6.1* was inserted in an intergenic region between the *Gr93a-d* cluster and the *gliolectin (glec)* gene. Insertion sites and orientations of the genetic donor lines are shown in **Supplementary Figure 4**.

Immunohistochemistry and imaging. Brains were dissected and fixed for 1 h in 2% paraformaldehyde in phosphate buffered lysine (50 mM lysine and 100 mM Na_2HPO_4; pH 7.4), then washed 3 × 5 min in PBST (137 mM NaCl, 2.7 mM KCl, 10 mM Na_2HPO_4, 2 mM KH_2PO_4 and 0.1% Triton X-100; pH 7.4). After the washes, the brains were blocked for 30 min in 10% normal goat serum in PBST and incubated with primary antibody overnight at 4 °C. Brains were then washed 3 × 5 min in PBST and incubated with secondary antibody for 2 h at room temperature (20–22 °C). After secondary incubation, the brains were washed 3 × 5 min in PBST and transferred to 70% glycerol. When staining for mCD8, the following primary and secondary antibodies were used: mouse anti-Bruchpilot (nc82)[47] (1:30, Developmental Studies Hybridoma Bank), rat anti-mCD8[17] (1:100, Invitrogen), goat anti-rat Alexa Fluor 488 (1:200, Molecular Probes) and goat anti-mouse Alexa Fluor 594 (1:200, Molecular Probes). When staining lines containing the *LexAop:rCD2-GFP* construct (and corresponding controls) chicken anti-GFP (1:2,000, Abcam) primary and goat anti-chicken Alexa Fluor 488 (1:200, Molecular Probes) secondary antibodies were used. Brains were mounted in Vectashield (Vector Laboratories) for imaging. Images were acquired on a Leica TCS SP2 AOBS confocal microscope with either a 20× (numerical aperture (NA) = 0.7) or 40× (NA = 1.25) lens. Confocal images were rendered in three dimensions using Imaris (Bitplane) and adjusted

doi:10.1038/nmeth.1561

as necessary in Photoshop (Adobe) using cropping and thresholding tools, and assembled into figures using Illustrator (Adobe).

InSITE reagents. *Drosophila* stocks, including the mobile, X-linked *P* element and *piggyBac* enhancer trap lines (*P{IT.GAL4}A134.3* and *PBac{IT.GAL4}0315*), the *y, w, hs-FLP, vas-ΦC31* line, and all of the genetic donor lines shown in **Supplementary Figure 4** have been deposited with the Bloomington *Drosophila* Stock Center. A collection of 100 InSITE enhancer trap lines is available upon request. All plasmids have been deposited with Addgene.

40. Gohl, D., Muller, M., Pirrotta, V., Affolter, M. & Schedl, P. Enhancer blocking and transvection at the *Drosophila* apterous locus. *Genetics* **178**, 127–143 (2008).
41. Schuldiner, O. *et al.* piggyBac-based mosaic screen identifies a postmitotic function for cohesin in regulating developmental axon pruning. *Dev. Cell* **14**, 227–238 (2008).
42. Hagstrom, K., Muller, M. & Schedl, P. Fab-7 functions as a chromatin domain boundary to ensure proper segment specification by the *Drosophila* bithorax complex. *Genes Dev.* **10**, 3202–3215 (1996).
43. Rubin, G.M. & Spradling, A.C. Genetic transformation of *Drosophila* with transposable element vectors. *Science* **218**, 348–353 (1982).
44. Potter, C.J. & Luo, L. Splinkerette PCR for mapping transposable elements in *Drosophila*. *PLoS ONE* **5**, e10168 (2010).
45. Ochman, H., Gerber, A.S. & Hartl, D.L. Genetic applications of an inverse polymerase chain reaction. *Genetics* **120**, 621–623 (1988).
46. Tweedie, S. *et al.* FlyBase: enhancing *Drosophila* Gene Ontology annotations. *Nucleic Acids Res.* **37**, D555–D559 (2009).
47. Wagh, D.A. *et al.* Bruchpilot, a protein with homology to ELKS/CAST, is required for structural integrity and function of synaptic active zones in *Drosophila*. *Neuron* **49**, 833–844 (2006).

Nature Methods

A versatile *in vivo* system for directed dissection of gene expression patterns

Daryl M Gohl, Marion A Silies, Xiaojing J Gao, Sheetal Bhalerao, Francisco J Luongo, Chun-Chieh Lin, Christopher J Potter & Thomas R Clandinin

Supplementary Figure 1	List of constructs used in the InSITE system
Supplementary Figure 2	Diversity of InSITE enhancer trap expression patterns in adult fly tissues and brains
Supplementary Figure 3	Validation of injectable InSITE plasmids
Supplementary Figure 4	Insertion sites and orientations of genetic donor lines
Supplementary Figure 5	Crossing schemes for performing swaps
Supplementary Figure 6	Eye colors are consistent for constructs integrated in the same enhancer trap landing site
Supplementary Figure 7	Analysis of the aberrant events seen in genetic swapping
Supplementary Figure 8	Additional functional tests of InSITE swaps
Supplementary Table 1	Antennal lobe glomerular innervation patterns of *PBac{IT.GAL4}3.1* and associated swaps
Supplementary Table 2	Oligonucleotides used for cloning in this study
Supplementary Table 3	PCR and sequencing primers used in this study

Nature Methods: doi:10.1038/nmeth.1561

Supplementary Figure 1

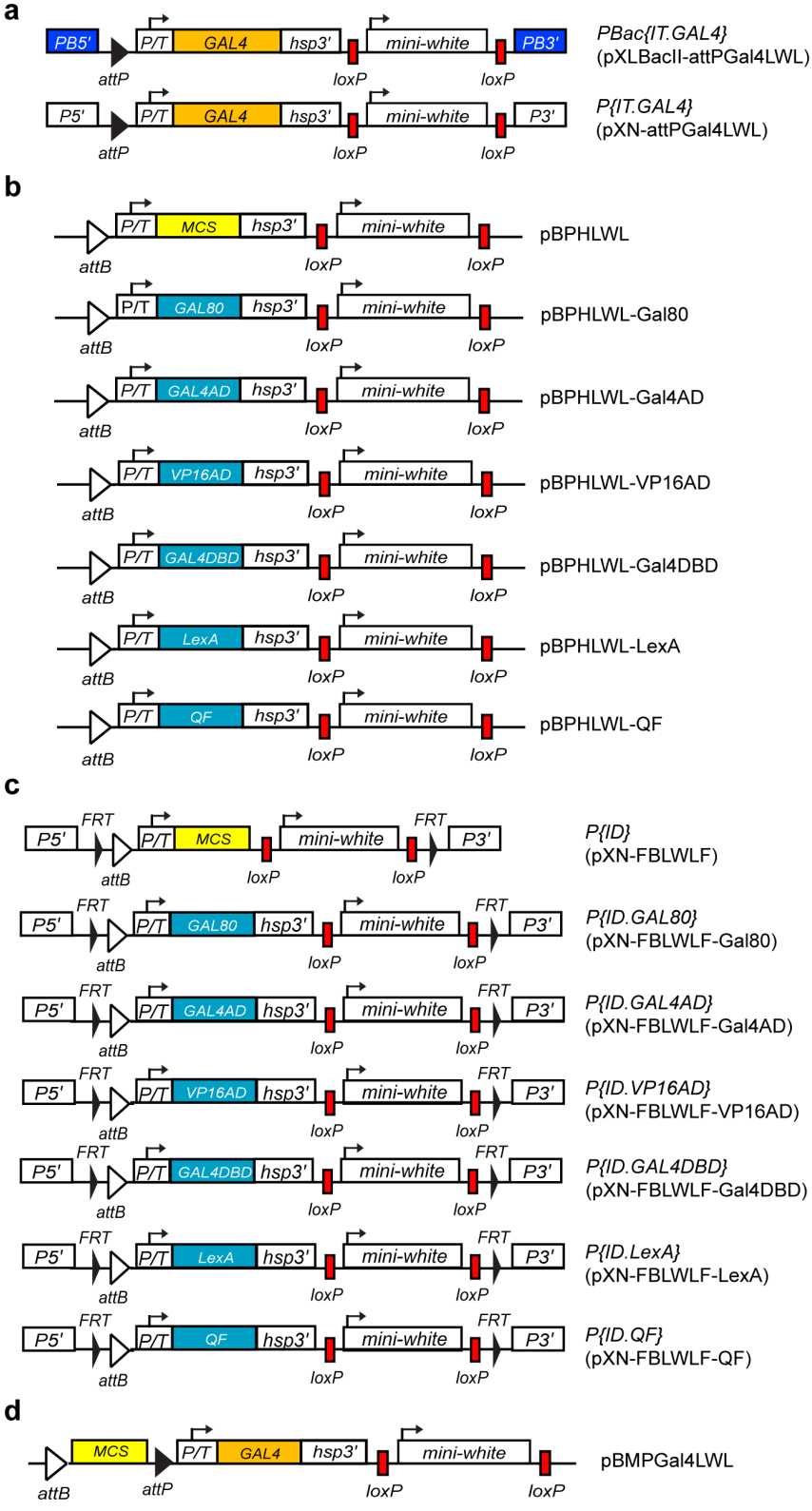

Nature Methods: doi:10.1038/nmeth.1561

Supplementary Figure 1

List of constructs used in the InSITE system. For constructs that also exist as transgenic lines, names of transgenes are listed, and DNA constructs used to generate the transgenic lines are noted in parenthesis. (**a**) Schematics of the two InSITE enhancer trap transposons. (**b**) Injectable donor plasmids. *pBPHLWL* is the injectable donor plasmid, with a multiple cloning site (MCS) that allows for insertion of desired effectors. (**c**) Genetic donor transposons. *XN-FBLWLF* is the donor transposon backbone, which contains a MCS. Multiple transgenic lines were established for all six donor constructs (**Supplementary Fig. 4**), and successful genetic swaps were carried out with all six elements. (**d**) The InSITE-compatible enhancer fusion vector, *pBMPGal4LWL*.

Nature Methods: doi:10.1038/nmeth.1561

Supplementary Figure 2

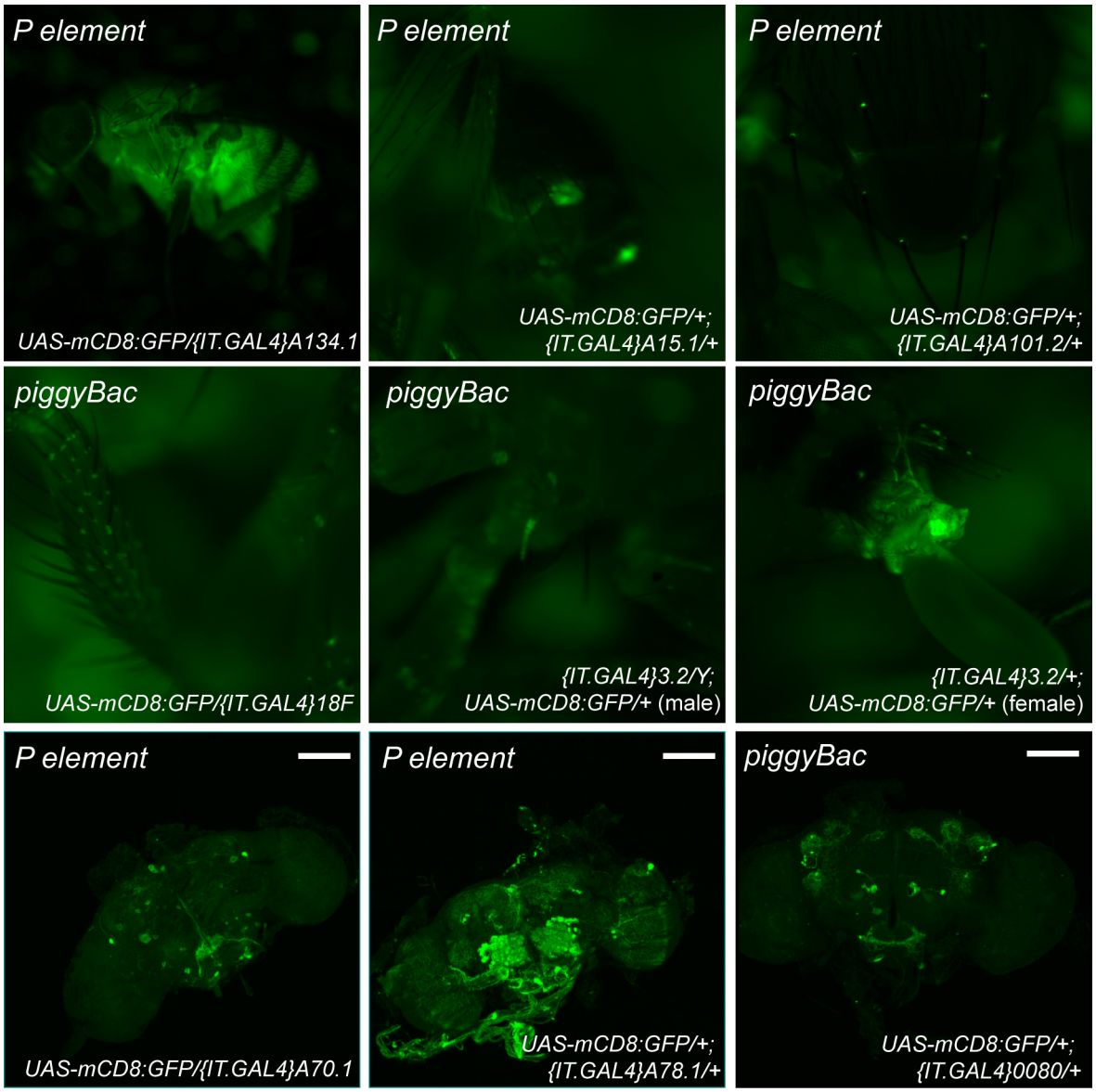

Supplementary Figure 2
Diversity of InSITE enhancer trap expression patterns in adult fly tissues and brains. mCD8:GFP expression is shown in green. Scale bar: 100 μm.

Nature Methods: doi:10.1038/nmeth.1561

Supplementary Figure 3

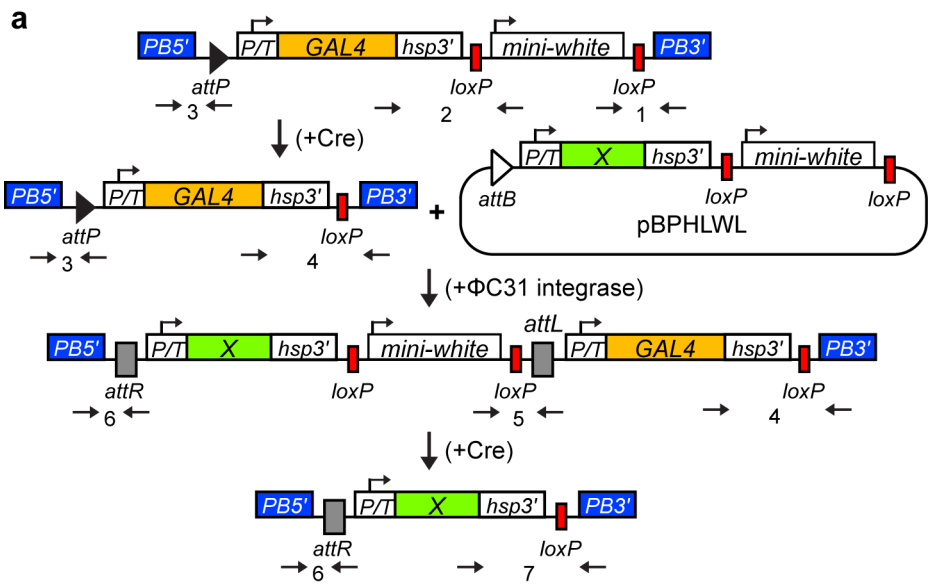

c

Donor construct	Injected into	Fertile crosses	Integration events	Integration rate (%)
pBPHLWL-GAL80	*{IT.GAL4.w-}6.1*	54	8	14.8
pBPHLWL-GAL4AD	*{IT.GAL4.w-}3.1*	91	20	22.0
pBPHLWL-VP16AD	*{IT.GAL4.w-}6.1*	60	12	20.0
pBPHLWL-GAL4DBD	*{IT.GAL4.w-}3.1*	84	8	9.5
pBPHLWL-LexA	*{IT.GAL4.w-}1.1*	34	4	11.8

Supplementary Figure 3

Validation of injectable InSITE plasmids (**a**) Swapping enhancer trap effectors by injecting a donor plasmid. ϕC31 integrase can be used to insert a microinjected *attB* donor plasmid (*pBPHLWL*), which is analogous to the circular genetic donor molecule shown in **Fig. 1b** into the

genomic *attP* landing site in the enhancer trap transposon. 1-7 indicate the positions of primers used to molecularly verify each construct.
(**b**) PCR results confirmed each step of the conversion of line *PBac{IT.GAL4}3.1* to the *GAL4DBD* hemi-driver. Primer locations are shown in panel (**a**). (**c**) Integration frequencies of different injected donor plasmids and landing sites.

Supplementary Figure 4

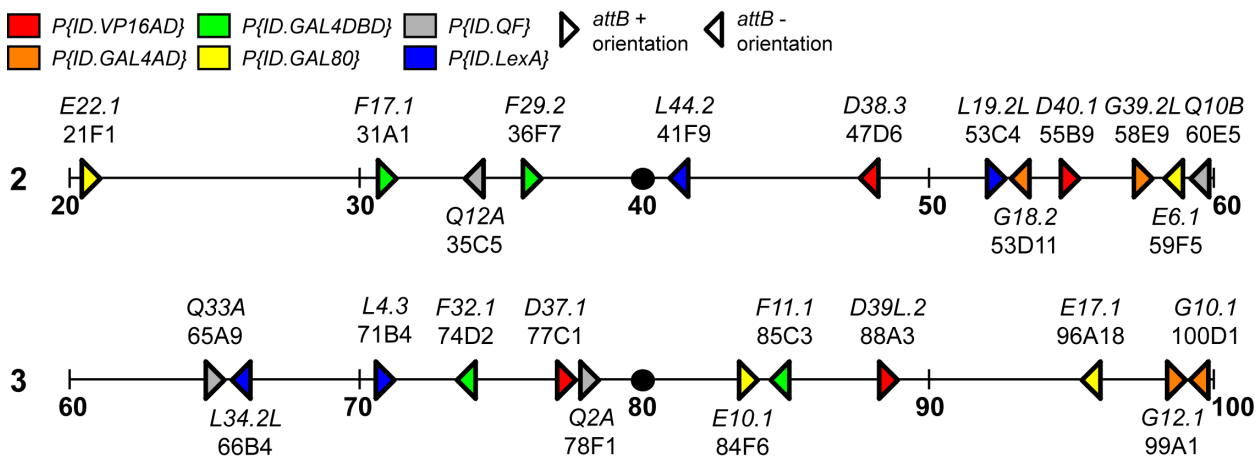

Supplementary Figure 4

Insertion sites and orientations of genetic donor lines on the second and third chromosomes.

Nature Methods: doi:10.1038/nmeth.1561

Supplementary Figure 5

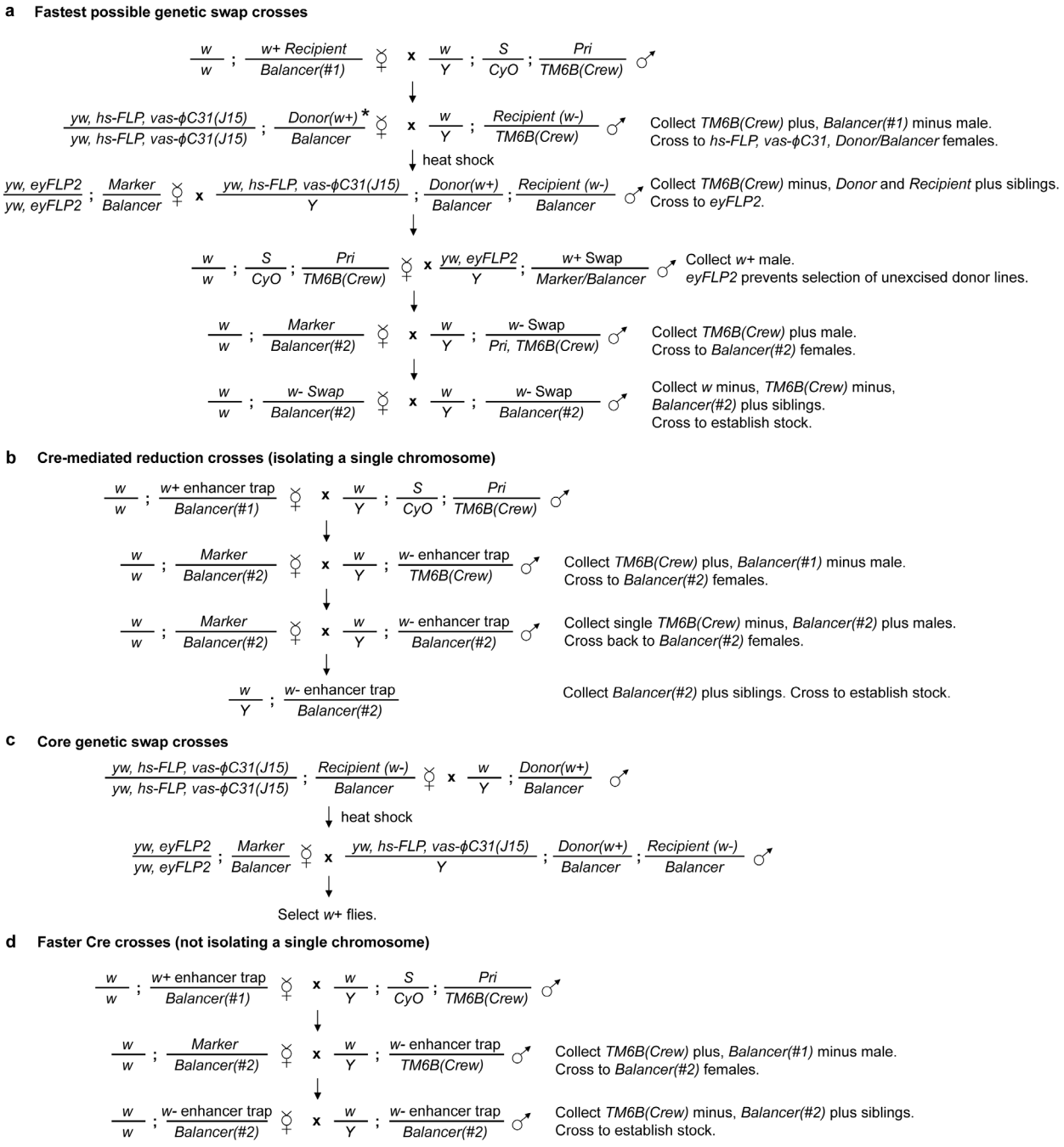

Supplementary Figure 5

Crossing schemes for performing swaps (see **Fig. 1b** and **Supplementary Fig. 3a**).
(**a**) Fastest possible crossing scheme for performing a genetic swap starting from an original, *mini-white*-containing InSITE enhancer trap line. Asterisk: while it is not recommended to maintain stocks containing both the *y, w, hs-FLP, vas-ϕC31* chromosome and a genetic donor

line over long time periods, due to degeneration of the donor chromosome, such a stock can be made fresh to facilitate the swapping of large numbers of enhancer trap lines to a single effector, or to speed up the crossing scheme when starting with *white*+ lines.
(**b**) Crossing scheme for Cre-mediated reduction steps. This is the cleanest way to do the Cre reduction, as it involves isolating a single Cre-treated chromosome and using this single chromosome to establish a stock. However, this may not be necessary as the Cre treatment step is highly efficient.
(**c**) Core genetic swap crosses. By selecting *white*+ flies in the final step that also contain the balancer chromosome or dominant marker that was opposite the donor chromosome in the previous generation, it is possible to eliminate aberrant events.
(**d**) Crossing scheme for Cre-mediated reduction steps in which a single chromosome is not isolated. Instead, two *white*- siblings are selected and crossed together to establish a stock. In this case, care should be taken to verify by PCR that the Cre excision went to completion on both chromosomes. However, we never detected an instance where this was not the case.

Supplementary Figure 6

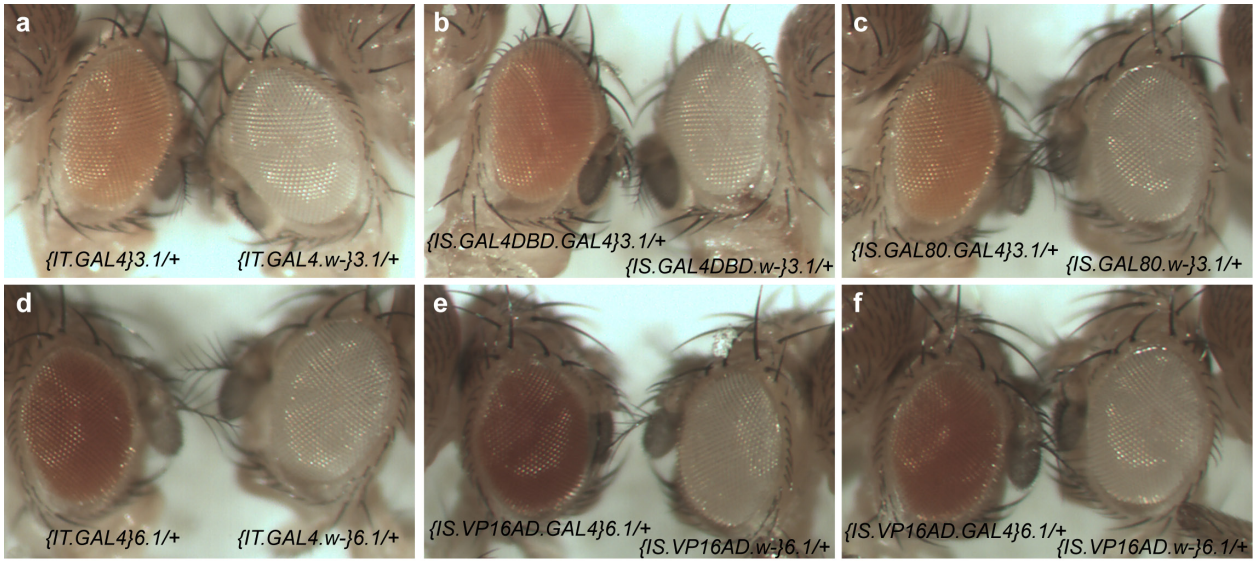

Supplementary Figure 6

Eye colors are consistent for constructs integrated in the same enhancer trap landing site. (**a**) Left: *PBac{IT.GAL4}3.1/+*, Right: *PBac{IT.GAL4.w-}3.1/+*. (**b**) Left: *PBac{IS.GAL4DBD.GAL4}3.1/+*, Right: *PBac{IS.GAL4DBD.w-}3.1/+*. Swaps generated by injection. (**c**) Left: *PBac{IS.GAL80.GAL4}3.1/+*, Right: *PBac{IS.GAL80.w-}3.1/+*. Swaps generated by genetic conversion using line *P{ID.GAL80}E17.1*. (**d**) Left: *PBac{IT.GAL4}6.1/+*, Right: *PBac{IT.GAL4.w-}6.1/+*. (**e**) Left: *PBac{IS.VP16AD.GAL4}6.1/+*, Right: *PBac{IS.VP16AD.w-}6.1/+*. Swaps generated by injection. (**f**) Left: *PBac{IS.VP16AD.GAL4}6.1/+*, Right: *PBac{IS.VP16AD.w-}6.1/+*. Swaps generated by genetic conversion using line *P{ID.VP16AD}D37.1*.

Supplementary Figure 7

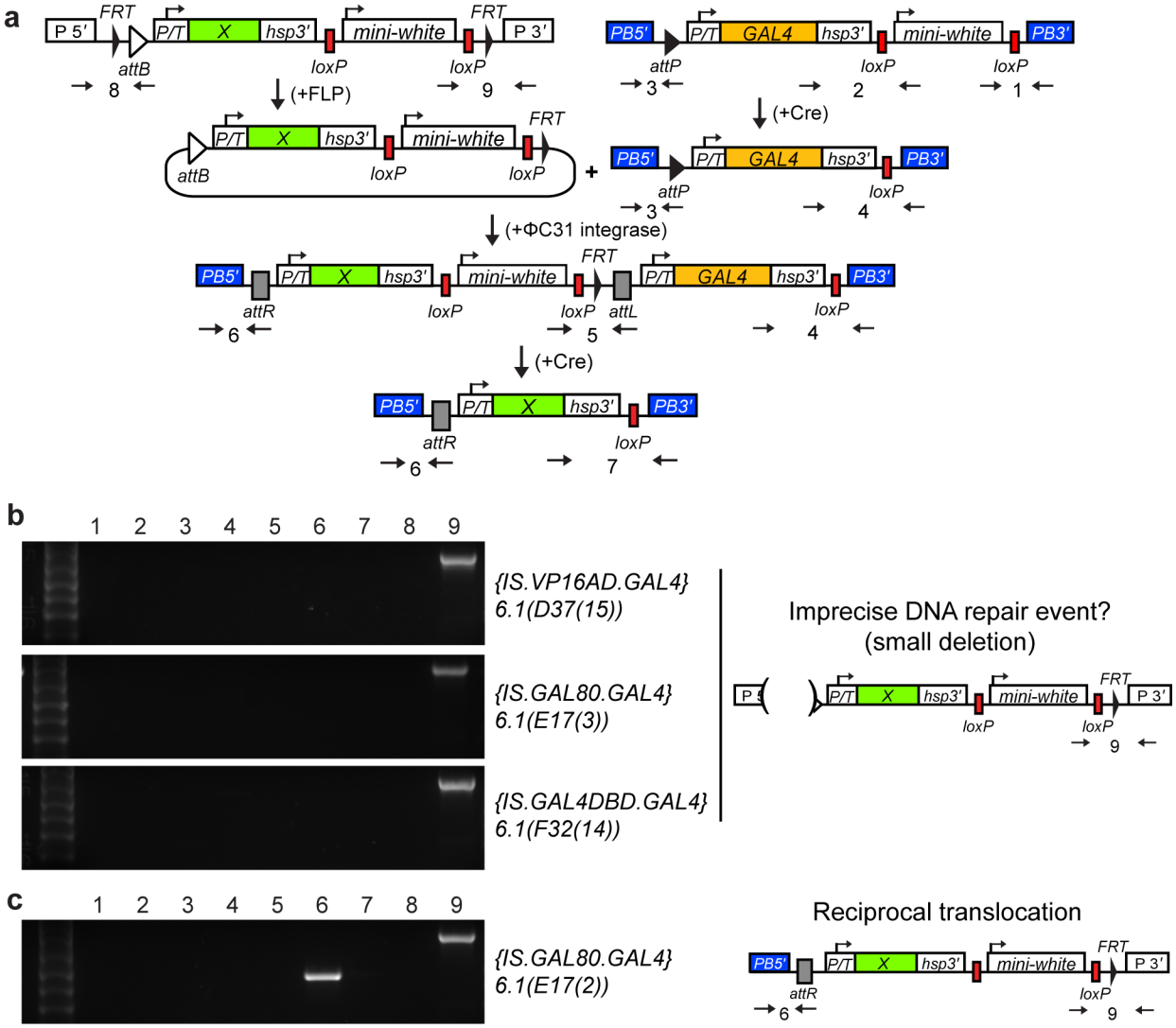

Supplementary Figure 7

Analysis of the aberrant events seen in genetic swapping. (**a**) Outline of genetic swap procedure. 1-9 indicate the positions of primers used to molecularly verify each construct. (**b**) This class of aberrant events displayed only a product for primer pair 9, indicating that the 3 ' junction of the genetic donor element was retained. The 5 ' end of the construct was not intact, and may have been subject to imprecise DNA repair[37], although other potential explanations, such as recombination with a pseudo *attP* site, are possible. (**c**) PCR tests indicating that *PBac{IS.GAL80.GAL4}6.1(E17(2))* was an event where the 3' junction of the genetic donor element remained intact, but in which the integration event took place between *attP* and *attB*, creating a reciprocal translocation between the donor and recipient chromosome.

Nature Methods: doi:10.1038/nmeth.1561

Supplementary Figure 8

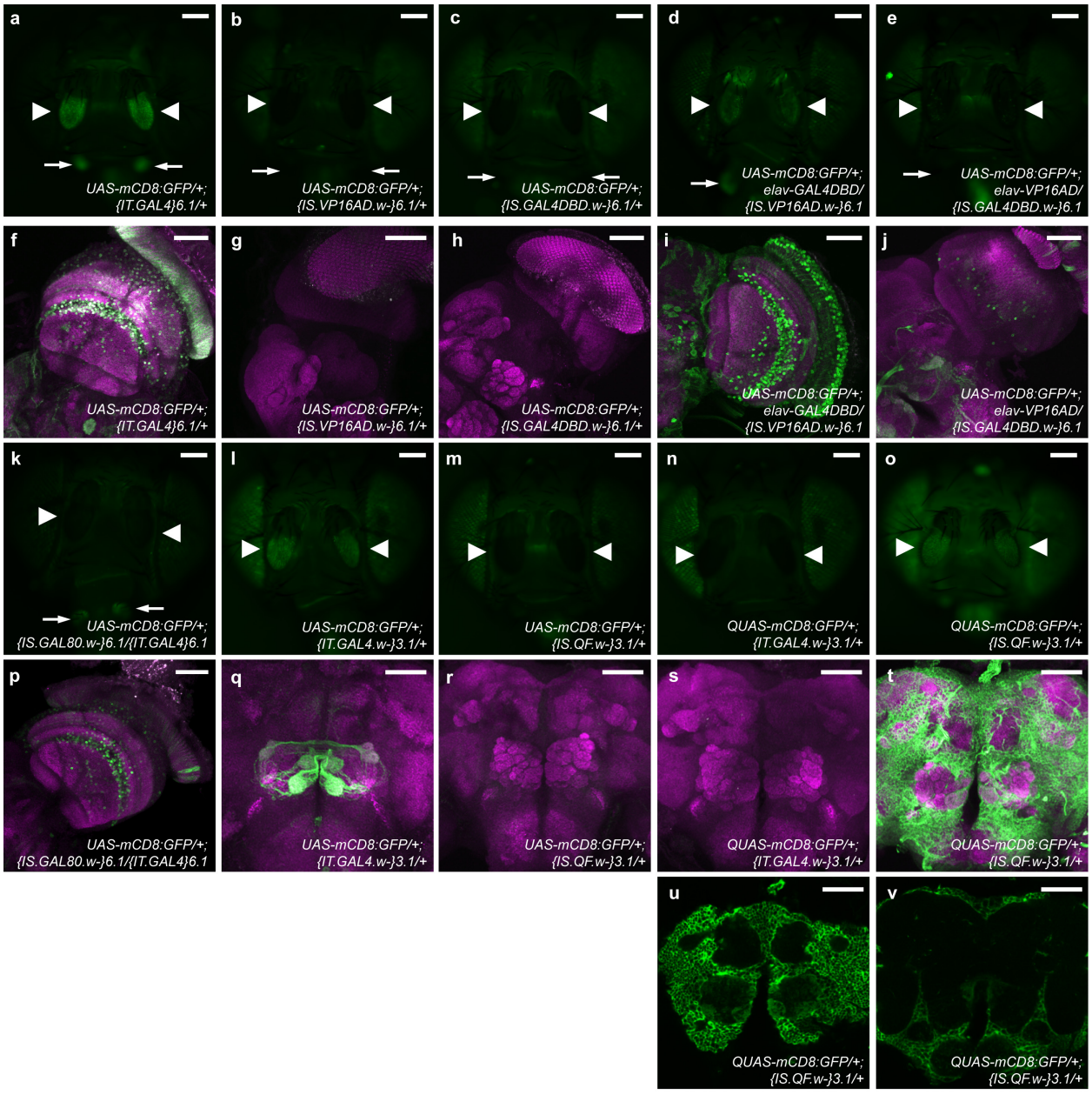

Supplementary Figure 8

Additional functional tests of InSITE swaps. (**a-e, k-o**) GFP expression in adult heads. Scale bar: 100 μm. (**f-j, p-t**) Adult brains stained with anti-mCD8 (green) and anti-Bruchpilot (nc82, magenta). Scale bar: 50 μm. *PBac{IT.GAL4}6.1* was expressed in the antennae (arrowheads) and maxillary palps (arrows) of adult flies (**a**), as well as in many other neurons and glia (**f**). No expression was seen in flies expressing only one half of split-*GAL4* (**b, c, g, h**). *PBac{IS.VP16AD.w-}6.1* /*elav-GAL4DBD* drove expression in a pattern similar to the original

Nature Methods: doi:10.1038/nmeth.1561

PBac{IT.GAL4}6.1 in the antennae and maxillary palps (**d**), and in the brain, with the exception of the lamina glial cells. (**i**). *PBac{IS.GAL4DBD.w-}6.1/elav-VP16AD* drove expression of CD8:GFP in only a small subset of the original *PBac{IT.GAL4}6.1* pattern both in the antennae (**e**) and in the brain (**j**). *PBac{IT.GAL4}6.1* expression was repressed by *PBac{IS.GAL80.w-}6.1* in the antennae, weakly in the maxillary palps (**k**) and in a subset of the neurons in the brain (**p**). Repression by *{IS.GAL80.w-}6.1* was strongest in lamina neurons and glia (**k**) and in the antennal lobes (not shown), and weakest in the medulla. No cross-talk was observed between *PBac{IT.GAL4.w-}3.1* and *QUAS-mCD8:GFP*, or between *PBac{IS.QF.w-}3.1* and *UAS-mCD8:GFP* (**m, n, r, s**). The *PBac{IS.QF.w-}3.1* swap recapitulated the pattern driven by *PBac{IT.GAL4.w-}3.1* in the antennae (**o**) and the antennal lobes (panels (**t-v**), also see Supplementary Table 1) but also included additional expression in a single glial subtype (cortex glia), as well as trachea (not shown). (**u, v**) mCD8 (green) channel of single slices of the image stack shown in panel (**t**).

Nature Methods: doi:10.1038/nmeth.1561

Supplementary Table 1

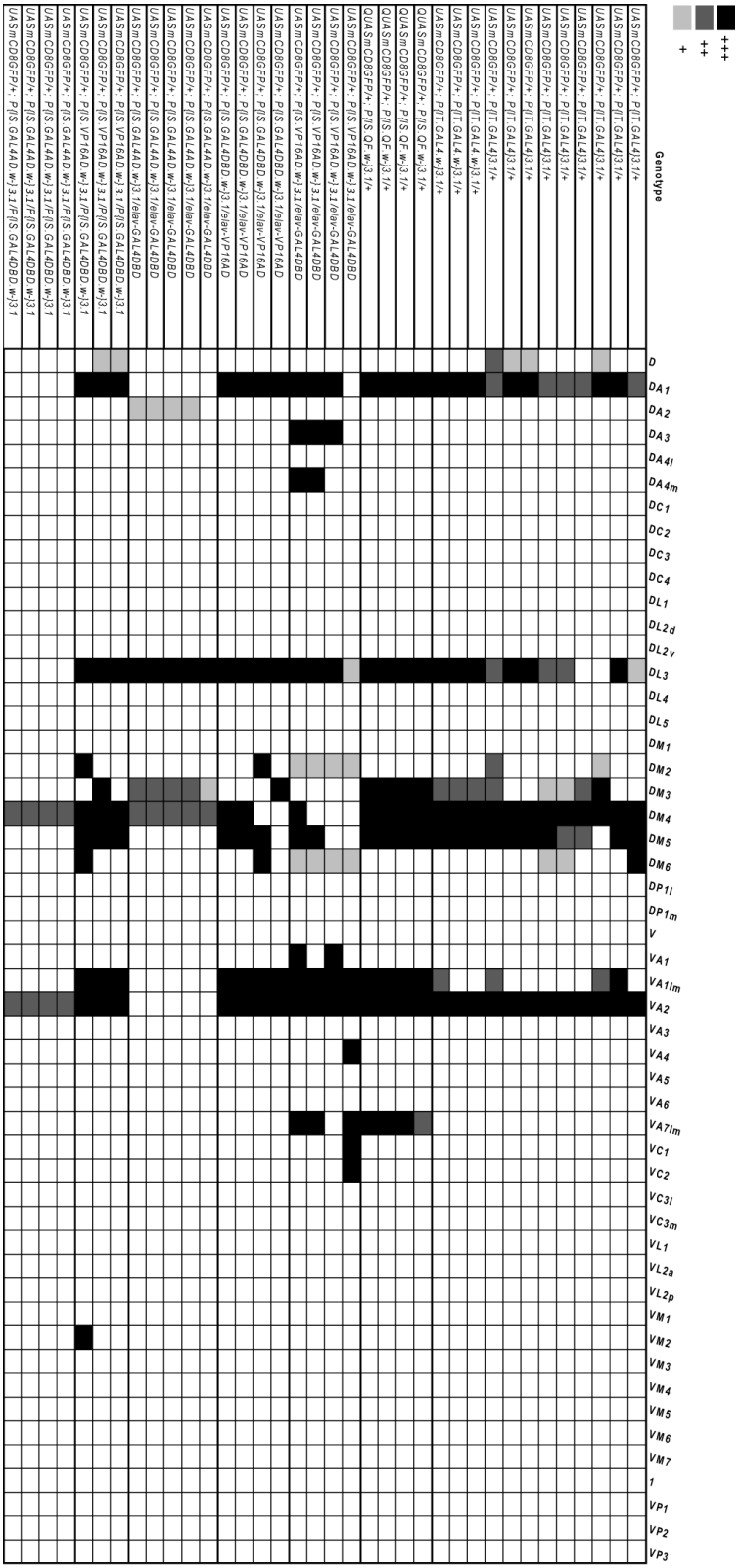

Nature Methods: doi:10.1038/nmeth.1561

Supplementary Table 1
Antennal lobe glomerular innervation patterns of *PBac{IT.GAL4}3.1* and associated swaps. Antennal lobe scoring was done blind to genotype. Expression intensity was divided into three categories: +++, strong; ++, weak; +, very weak.

Nature Methods: doi:10.1038/nmeth.1561

Supplementary Table 2

Name	Sequence
SPpolyF	TTAATTAAGCGGCCGCTGCA
PSpolyR	GCGGCCGCTTAATTAAAGCT
HKpolyF	AGCTTCTAGAGGATCCACTAGTGAGCTCGGTAC
KHpolyR	CGAGCTCACTAGTGGATCCTCTAGA
Oligo 1F	CAAGCTTGGATCCGCGGCCGCACGCGTGGCGCGCCT
Oligo 1R	CTAGAGGCGCGCCACGCGTGCGGCCGCGGATCCAAGCTTGGTAC
Oligo 2F	CTAGATCGATGCTAGCTTAATTAAGCATGCACTAGTAGATCTGAGCT
Oligo 2R	CAGATCTACTAGTGCATGCTTAATTAAGCTAGCATCGAT
5'FRT(Kpn)F	CGAAGTTCCTATACTTTCTAGAGAATAGGAACTTCGGCGCGCCAGTAC
5'FRT(Kpn)R	TGGCGCGCCGAAGTTCCTATTCTCTAGAAAGTATAGGAACTTCGGTAC
3'FRT(Not-Sac)F	GGCCGCGCTCTTCCGCTGAAGTTCCTATACTTTCTAGAGAATAGGAACTTCCTCGAGCT
3'FRT(Not-Sac)R	CGAGGAAGTTCCTATTCTCTAGAAAGTATAGGAACTTCAGCGGAAGAGCGC
GC NotI F(dXho)	GGCCGCGATATCTTAATTAAGCATGCCTAGGCTAGCACGCGTAGATCT
GC NotI R(dXho)	GGCCAGATCTACGCGTGCTAGCCTAGGCATGCTTAATTAAGATATCGC
Pst-Sac EF Linker For	GCTAGCTTAATTAAGATCTGGCGCGCCGCGGCCGCAAGCTTGAGCT
Pst-Sac EF Linker Rev	CAAGCTTGCGGCCGCGGCGCGCCAGATCTTAATTAAGCTAGCTGCA

Supplementary Table 2
Oligonucleotides used for cloning in this study.

Supplementary Table 3

Name	Sequence
9-1	GACCTGTTCGGAGTGATTAGCGTT
attBR1	ATACCGTCGACCTCGACAT
attPR1	CACAACCCCTTGTGTCATGT
BHI-QF-FOR	TAAAGGATCCAAAATGCCGCCTAAACGCAAG
FLP Set 1 Forward Primer	AAGTGAGGGTGAAAGCATCTGGGA
FLP Set 1 Reverse Primer	AGTCAACTCCGTTAGGCCCTTCAT
FLP Set 2 Forward Primer	AGGTGCTTGTTCGTCAGTTTGTGG
FLP Set 2 Reverse Primer	TCCCAGATGCTTTCACCCTCACTT
Gal43'F2	CTTGGCCATGTAACCTCTGAT
Gal4AD 3'F1	GGAGGTGGAGGTACTAGTCT
Gal4DBD 3'F1	GCCTCTAACATTGAGACAGCAT
Gal80 3'F1	CACCTTGATGGATGCTCTGATA
Gal80F1(seq)	CTCAAGGCTATATCGGCGACA
Gal80R1(seq)	ACAGGCCTTTCGTAGCCGTA
hsp3'F	GATACCGTCGACTAAAGCCAA
hsp3'R(seq)	CTTTTGGTTGGTTACAACCAA
hsp70-FOR-QF-LNKR	TAAGCACTAGTGCAGATCTTATCGATACCGTCGACTAAAGCC
LexA 3'F1	CCATGGGGAATGGTTTATGGTT
LexA1F	GTCGTAGATCTTCGTCAGCAGA
LexA1R	TCCTCGCCGTCTAAGTGGAGCT
M13For	GTTGTAAAACGACGGCCAGT
M13Rev	TCACACAGGAAACAGCTATGA
MW2F(seq)	GCTGCATTAACCAGGGCTTC
MW2R(seq)	GGTGAGGTTCTCGGCTAGTT
MW3'F	CTCAAATGGTTCCGAGTGGTTC
MW3F(seq)	TTCGCCTCCGAGGCTCTAA
MW3'F2	CTCCGCAACACATTCACCTT
MW3R(seq)	CTGCGACAGCTTCTTCAGCA
MW4F(seq)	CGAATATTAATGAGATGCGAGT
MW4R(seq)	CACACCCACTTGCGTGAGTT
MW5'F(seq)	CGCTGTTTGCCTCCTTCTCT
MW5'R	GCGAAAGAGACGGCGATATT
MW5'R2	CGATCTCTCGTGGGATCATTG
MW6F(seq)	CCAGTTCGGGCAAGGTCAT
MW6R(seq)	CCAAAGTCTACTTGTGGGGAT
MWUp300	GACGCAGCGGCGAAAGAGA
ortc2 5'R	CAGAGGGAAATCGCAAGGAA
ortc2b For	GCGGCCGCGGTACCTTGGAGCATCTTGCACTT
ortc2b Rev	GAGGATCCGTTGGTGGCGAA
P3'Rnew2R	CCGTGGGGTTTGAATTAACTCA
P5'inF	GTGCGTTAGGTCCTGTTCAT
PBac3'R4	CGCATGTGTTTTATCGGTCTGT
PBac5'F1	ACCCAATTCGCCCTATAGTGA

pBSF1	GATTTAGAGCTTGACGGGGAA
pGaTn-hsp70REV-NotI-BH1	TATTTGGATCCGCGGCCGCGGATCTAAACGAGTTTTTAAGCAAACTCACTCCC
pPromF	GAGTACGCAAAGCTTACCGAA
pPromF(seq)	CAGTGCACGTTTGCTTGTTGA
pPromR	TTGGATCCACGTAAGGGTTAATGTT
QF 3'F1	GATCCGCAGTTCATGACGAA
QFREV-hsp70-LNKR	GTATCGATAAGATCTGCACTAGTGCTTACTATTGCTCATACGTGTTGATATCGC
yellow 3'F2	CCTACACACGGTACTTGGGTA

Supplementary Table 3
PCR and sequencing primers used in this study.